END
DATE
FILMED
9-79
DDC

1.0

4.5
5.0

2.8 2.5

3.2 2.2

3.6

1.1

4.0 2.0

1.8

1.25 1.4 1.6

MICROCOPY RESOLUTION TEST CHART
NATIONAL BUREAU OF STANDARDS 1963 A

NRL 541298

LEVEL

①

SC

ORIGINAL CONTAINS COLOR PLATES: ALL DDC
REPRODUCTIONS WILL BE IN BLACK AND WHITE.
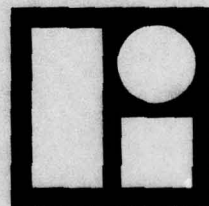
Litton

ELECTRON TUBE DIVISION

79 08 20 081

(1)

(6)

FEASIBILITY DEMONSTRATION
OF A
HIGH POWER WIDEBAND TWT
WITH LOW AM/PM DISTORTION.

(15) Contract N00173-77-C-0214

(9) FINAL REPORT,

CLIN 0002

Exhibit A, CDRL Item A003

NRL # 541298

D D C
RECEIVED
AUG 22 1979
C
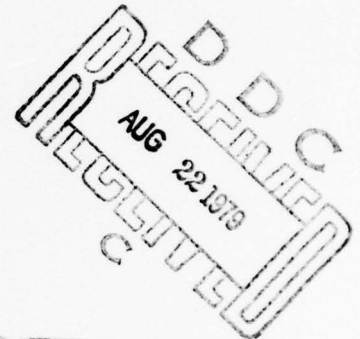
(11) 26 Feb 79

LITTON SYSTEMS, INC.

dba Litton Industries

Electron Tube Division

960 Industrial Road

San Carlos, California 94070

(12) 59 p'

125 170

Prepared By: _____

(10) E. G. Chaffee — Project Engineer

Approved By: _____

B. J. Hamak — Chief Engineer

Prepared For:

Naval Research Laboratory

Scientific Officer, Mr. R. Van Wagoner/Code 5252

Washington, D. C. 20375

February 26, 1979

125 170

TABLE OF CONTENTS

i

LIST OF FIGURES

1.0 INTRODUCTION

Loss-line stabilized tubes have been under development at Litton Industries under the supervision of the Naval Research Laboratories since 1973.

Early developmental tubes demonstrated high power, wide bandwidth and efficient operation. In-band distributed loss techniques were developed to form attenuator sections to provide lower bandedge stability and to allow efficient operation at the high frequency bandedge. Stabilization problems, however, at the upper bandedge prevented operation at full design perveance. In the last tube preceding this Contract, upper bandedge stability techniques were improved significantly; but, the tube exhibited in-band regenerative oscillations which prevented direct demonstration of this stability improvement.

The two tubes built under this Contract both demonstrated oscillation stability at design perveance and fully demonstrated the potential of loss line stabilized tubes. The design changes and the demonstration of these two tubes as discussed in this report.

In addition to stability considerations there was an additional effort to study AM-PM conversion in wideband coupled cavity tubes. Calculations are presented which show that low AM-PM can be obtained over a considerable portion of the hot bandwidth. Design changes were implemented in these tubes to minimize AM-PM conversion. Lower AM-PM conversion was demonstrated on these tubes than on comparable loss button tubes.

- 1 -

Table I shows typical electrical and RF parameters for the L-5631 loss line stabilized coupled cavity TWT.

L-5631 - Loss Line Stabilized CCTWT
Typical Electrical And RF Parameters

Cathode voltage	32.0 kV
Cathode current	6.5 amperes
Grid pulse voltage	300 volts
Grid bias voltage	-500 volts
Filament voltage	10.5 volts
Filament current	5 amperes
Collector voltage	10.6 kV
Power output	20 kW
Frequency	7 - 11 GHz
Gain	36 dB min.
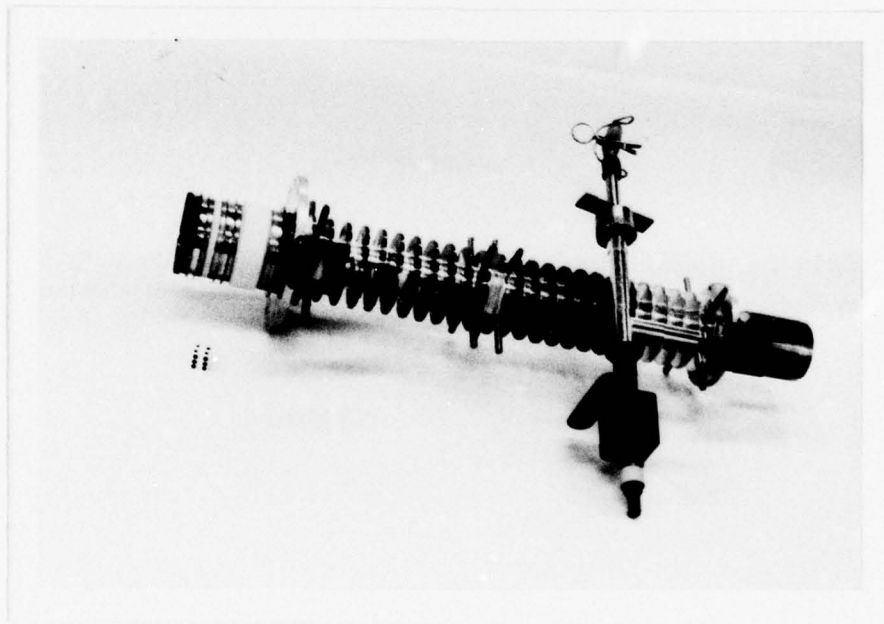
2.0 AM-PM CALCULATIONS

AM-PM conversion is the incremental increase of total
phase shift through the tube for an incremental drive
power change. It is zero in the small signal or linear
region and non-zero in the large signal or non-linear
region.

The dependence of AM-PM on the tube parameters, b, QC,
C and d was investigated using a large signal computer
program[21]. This program was written by Dr. J. R. M.
Vaughan of Litton Industries and has been published in
the IEEE Transactions. It has since been modified to
include absolute phase. The program essentially calculates
the power, gain, phase, etc. in a cavity by cavity sequence
through the tube. The electron beam is modeled by a beam
segment having one RF period which is subdivided into
12 disks of charge. The parameters b, QC, C and d are
calculated from Pierce's theory and are calculated for
reference only. They are not used in the large signal
calculations.

The program in general works quite well in modeling tubes
up to saturation, but does not work satisfactorily beyond
saturation in the overdrive region. We were, however, most
interested in studying the near saturation region where
the nonlinearity process begins and, therefore, for this
region the program was adequate.

The dependence of AM-PM on the synchronism parameter b
was investigated using a long section of circuit with no
attenuator and no sever. In practice the tube would
oscillate but this fact is unimportant for the calculations.
It was important not to allow sever or attenuator effects
to influence the results.

The circuit investigated was the broadband type used in
the loss line tubes. Figure 1 shows the unloaded ω-β
diagram for this circuit. The circuit is coalesced
at 12 GHz so that no stop band exists between the
passband and the slot mode. The hot band is from 7 GHz
to 11 GHz. Cold test data for this circuit was used
in the calculations for AM-PM conversion.

Figure 2 shows the results of the computer analysis at
midband (9 GHz). AM-PM conversion is shown plotted
against power output for several values of the synchro-
nism parameter b. For low power output the AM-PM
conversion is low regardless of the value of b. This
corresponds to the small signal region. In the large
signal region the AM-PM conversion increases and,
depending on the value of b, can be quite large. In
the upper right corner of Figure 2 the small signal gain
per cavity is shown as a function of the synchronism
parameter b. For values of b greater than b_0, the value
of b for maximum gain, both the AM-PM conversion and the
efficiency are high. As b is decreased there is a region
of b in which the AM-PM conversion is minimum. For
midband the maximum AM-PM from small signal to saturation
is about $2°/dB$ in this region $(1 \leq b \leq 1.5)$. For low
values of b the AM-PM conversion is large and the efficiency
is low. The AM-PM conversion also changes sign indicating
a shorter tube phase length. It is also interesting to
note that for high efficiency operation the maximum AM-PM
occurs at saturation while for an undervoltaged condition, the
maximum AM-PM occurs before saturation.

Figure 3 shows the computer results for the lower bandedge
of the tube. At this frequency the circuit impedance

- 4 -
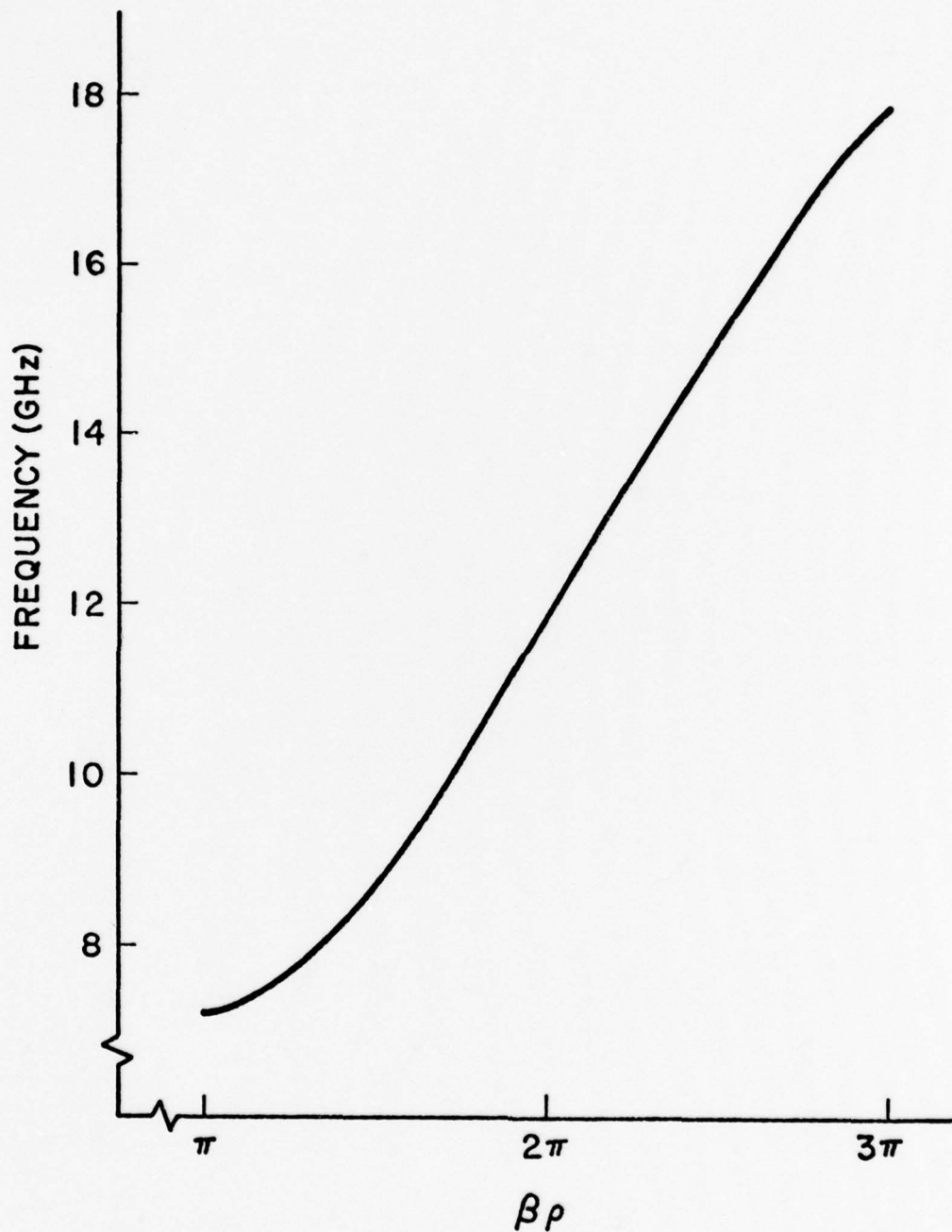
L-5631 ω-β DIAGRAM (UNLOADED)

FIG. 1
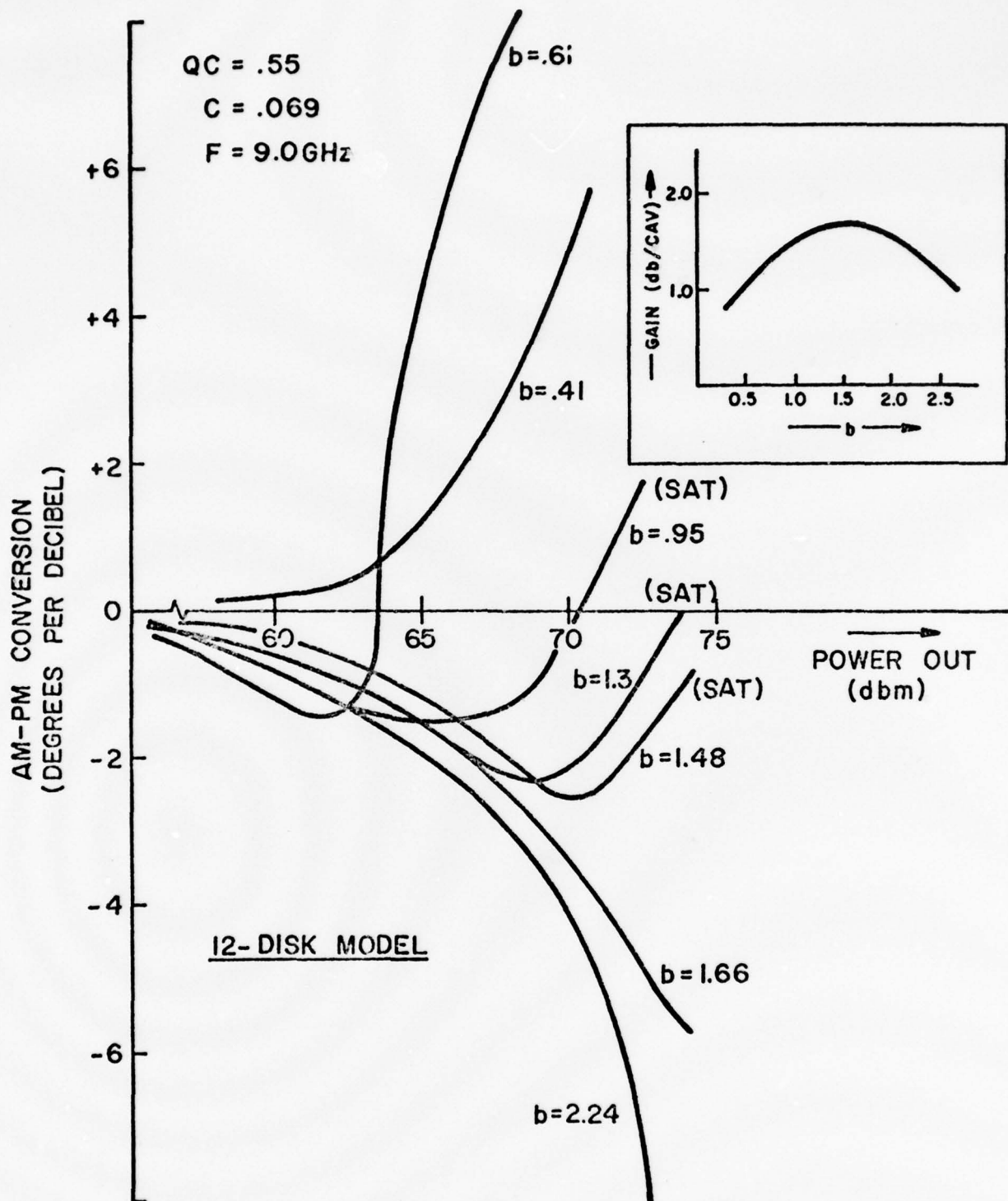
AM-PM CONVERSION VS. POWER OUTPUT
SYNCHRONISM PARAMETER VARIABLE.
(MIDBAND)

FIG. 2

- 6 -

QC = .192
C = .12
F = 7.5 GHz

AM–PM CONVERSION
(DEGREE / DECIBEL)

GAIN (dB / CAV) →

b →

b = –.34
b = – .17
b = 0
b = .95
b = 1.5

12-DISK MODEL

AM–PM CONVERSION VS. POWER OUTPUT
SYNCHRONISM PARAMETER VARIABLE.
(LOWER BANDEDGE)

FIG. 3

is high and the value of C is almost double that at midband. The AM-PM conversion is minimum near b = 0 and is less than 1°/dB over the drive range from small signal to saturation. The improved AM-PM characteristics at the lower bandedge are due to the high value C and the low value of QC. The circuit is highly under-voltaged at this frequency, bu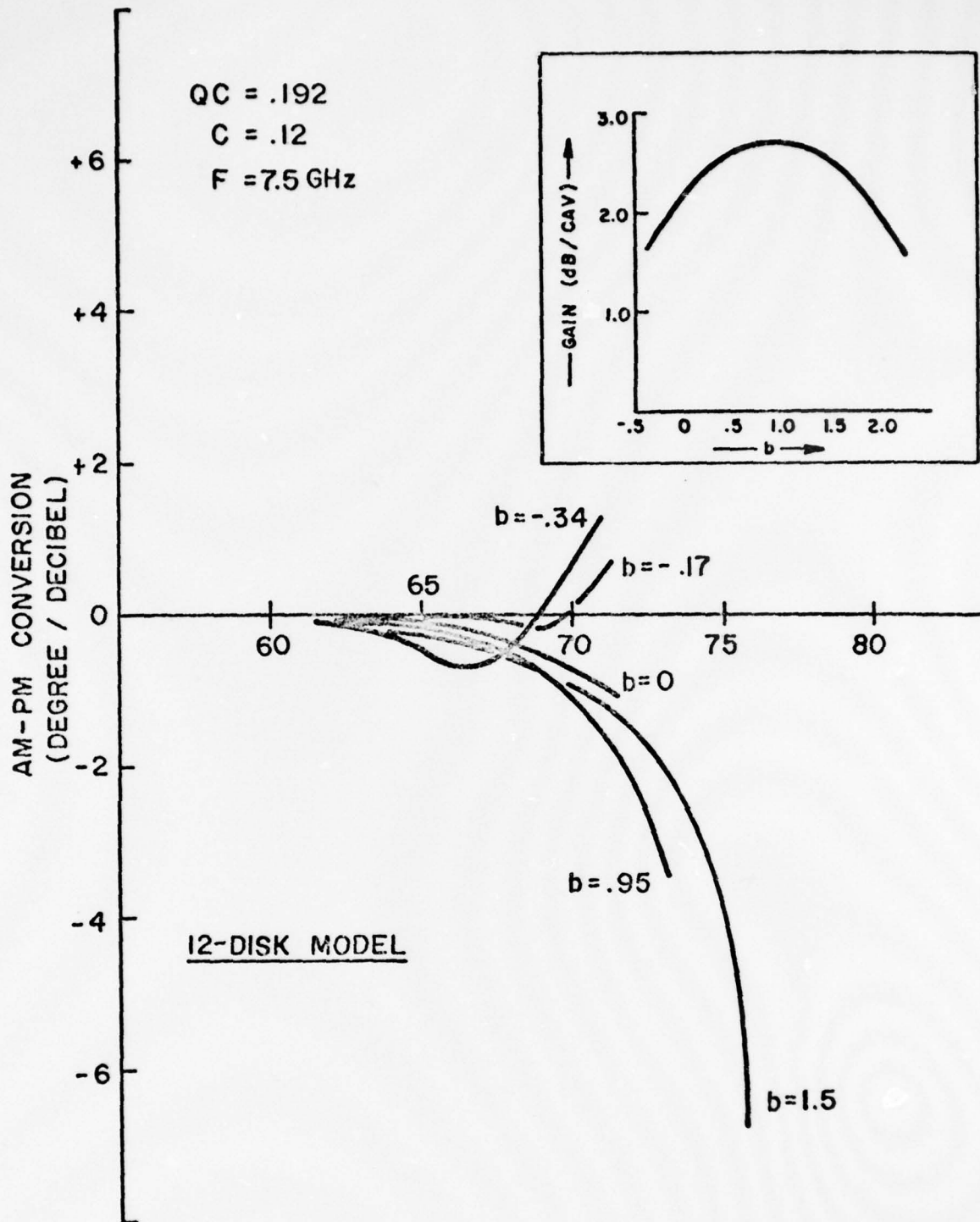t the efficiency is still reasonable although much lower than it could be for an overvoltaged condition. The minimum AM-PM voltage at the lower bandedge is the same voltage for which the minimum occurs at midband. This somewhat unexpected result leads to the conclusion that a minimum AM-PM can be obtained over a large percentage of the total band-width.

Figure 4 shows the AM-PM conversion versus power output for the upper frequency bandedge. The impedance is low at this frequency and the corresponding value of C is low and the value of QC is quite high. The best AM-PM at a reasonable efficiency occurs just below the maxi-mum small signal gain at about b = 1.36. Better values of AM-PM occur for lower values of b, but the efficiency falls off dramatically. The maximum AM-PM occurs at saturation in this case.

The best AM-PM values occur across the band at about 30 kV. Figure 5 shows the optimum AM-PM as a function of frequency at this voltage. It can be seen that the AM-PM values increase with frequency and the best results are obtained at the lower bandedge.

Computer runs were made to determine the dependence of AM-PM conversion on the loss parameter d. Figure 6 shows the AM-PM conversion as a function of power output

- 8 -
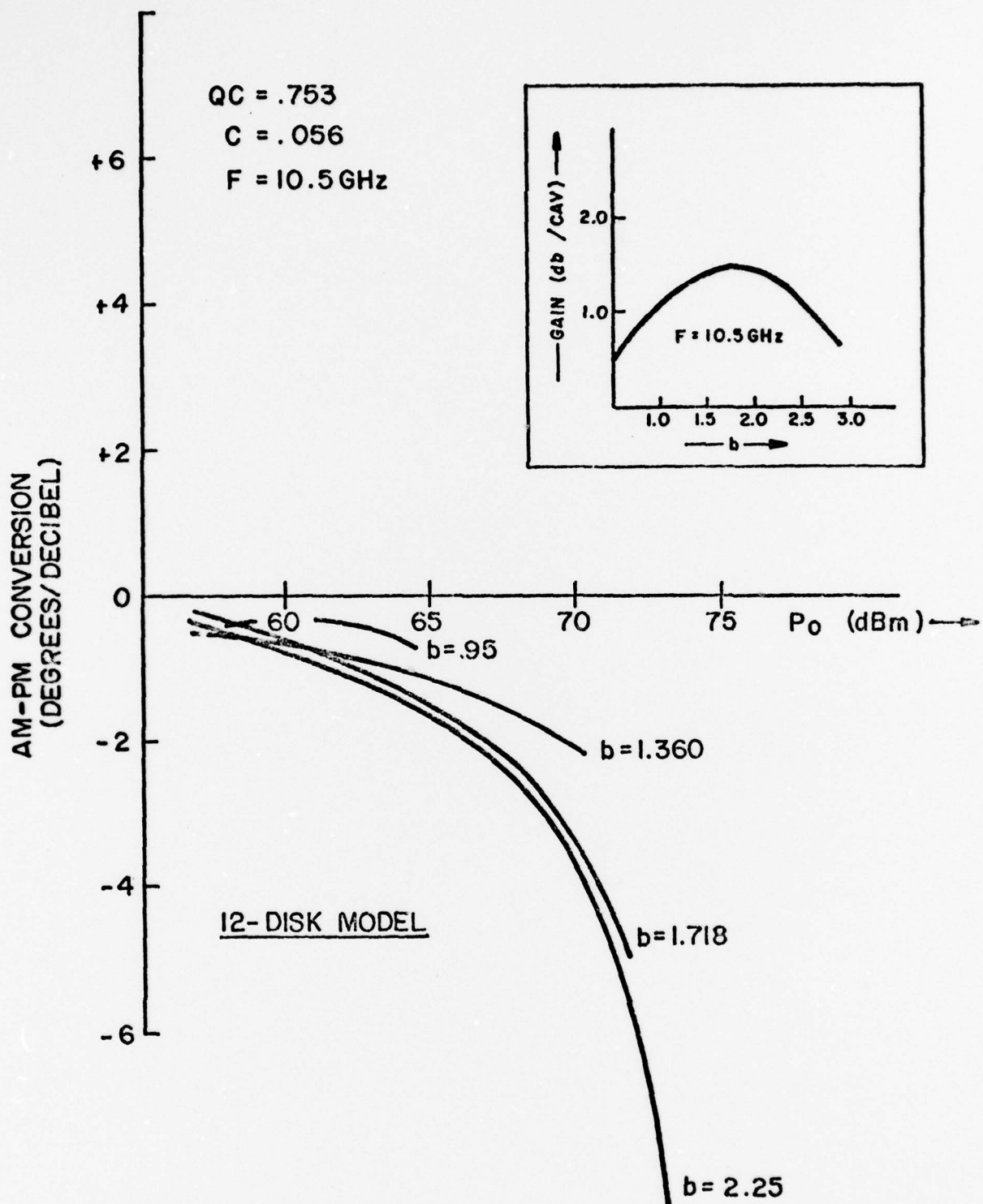
AM-PM CONVERSION VS. POWER OUTPUT
SYNCHRONISM PARAMETER VARIABLE.
(UPPER BANDEDGE)

FIG. 4
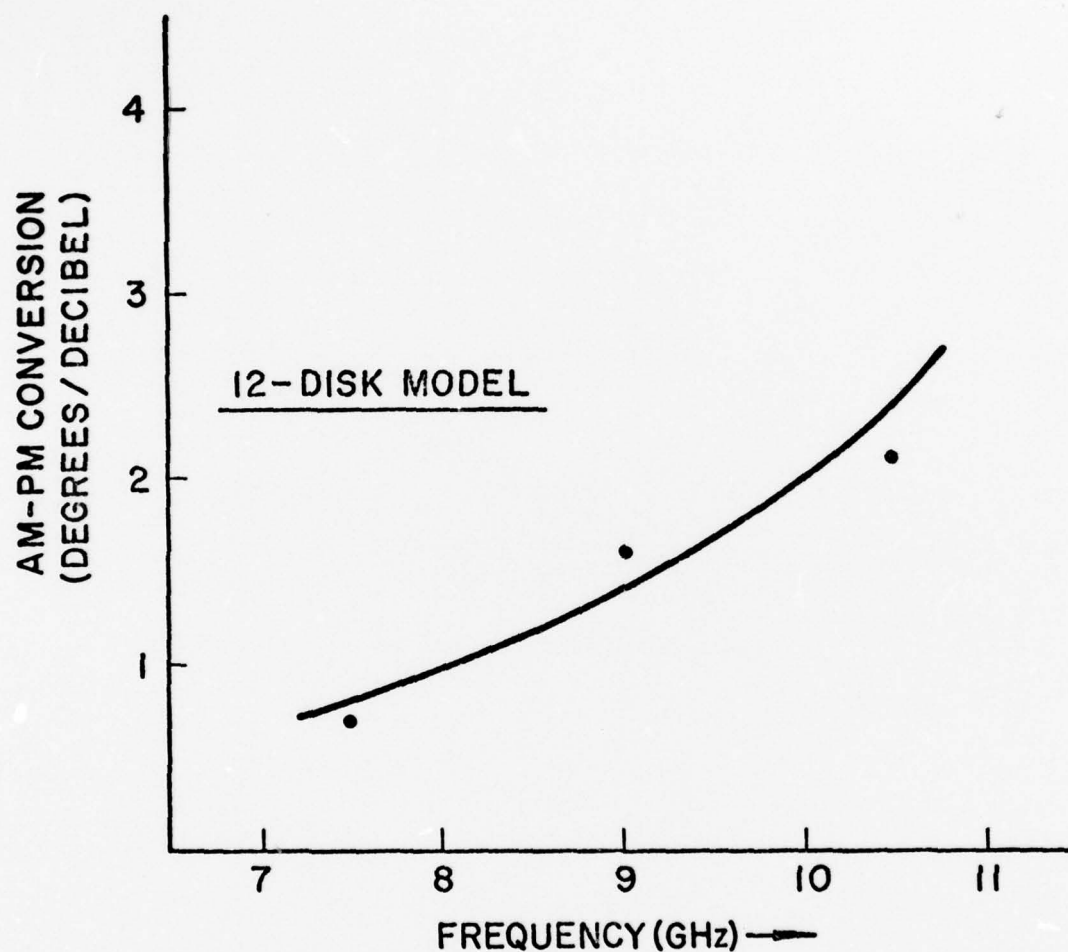
OPTIMUM AM-PM VS. FREQUENCY

FIG. 5

- 10 -

QC = .192
C = .12
F = 7.5GHz
b = 0

12-DISK MODEL
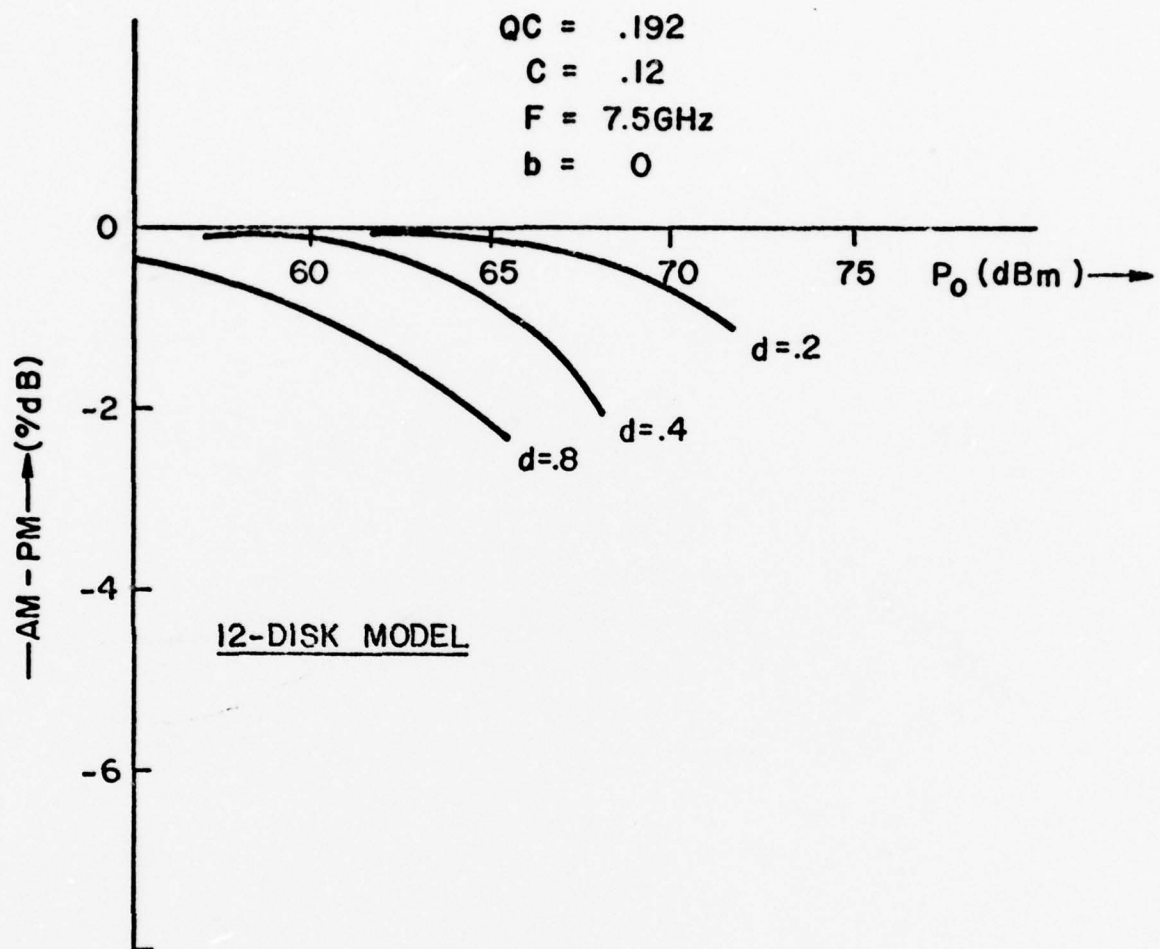
**AM-PM CONVERSION VS. POWER OUTPUT
LOSS PARAMETER VARIABLE**

FIG. 6

for three values of the loss parameter. The calculations
were made at the lower bandedge at the AM-PM minimum
(b = 0). For d = .2 the calculated AM-PM was less than
1°/dB. Doubling the circuit loss (d = .4) doubles the
AM-PM conversion and also results in a loss of efficiency.
Further increase of the loss increases the AM-PM conver-
sion at the same output power and reduces the efficiency
of the tube. Therefore, the loss in the power section of
the tube must be kept minimum. For a PPM focused tube
all pole pieces should be copper plated for minimum re-
sistivity. No distributed loss should be intentionally
introduced to the power section.

Additional computer runs were made to determine the optimum
positions of the attenuator in the output section for best
AM-PM results. The best results were obtained as expected
with the attenuator close to the sever and as far as
possible from the tube output. In general good results
were obtained when the length of the power section was
sufficient to yield 15 - 20 dB small signal gain. This
agrees with results published by Ober[11] and Nishihara[17].

In conclusion, the best AM-PM circuit design is also the
best circuit design for efficiency. Impedance should be
maximized to obtain a maximum value of C. This insures
QC is low since QC $\propto$ $1/C^2$. Also, the loss parameter d
should be minimized. The best AM-PM values occur when the
tube is undervoltaged. The best efficiency is obtained
for an overvoltaged condition.

- 12 -

3.0   DESIGN MODIFICATION

3.1   Stabilization

The upper cutoff instability problem, manifested by
the early loss line tubes, was solved in these tubes by
increasing the loss per cavity at upper cutoff and by
including loss in nearly every cavity of the tube. The
cavities in the bellows and weld seal regions (8 total
cavities) cannot be loaded since they cannot be directly
exposed to the lossy ceramic.

Two loss lines were used to obtain the desired characteristics
for the upper cutoff loss. A very high "Q" design was used
to suppress the oscillation while not "spilling" loss into
the operating band.

The distributed loss attenuation was provided by two addi-
tional loss lines oriented at 180° to each other. Since
the attenuators are confined near the sever this loss is
not added to every cavity in the tube. Two loss lines were
used to form the attenuator since the perturbations to the
circuit are rather large for this type of loading and an
uneven loading will accentuate mismatches around the $\beta p = 3\pi/2$ frequency.

In all, there were four loss lines used to stabilize the
tube — two for upper cutoff and two for the distributed
loss attenuator. These are oriented as shown in Figure 7
at 90° to each other.

3.2   Loss Rod Fabrication

Figure 8 shows how the loss rods were fabricated for this
design. The high "Q" construction is used for the upper
cutoff stabilization. A thin stripe of loss is used

- 13 -
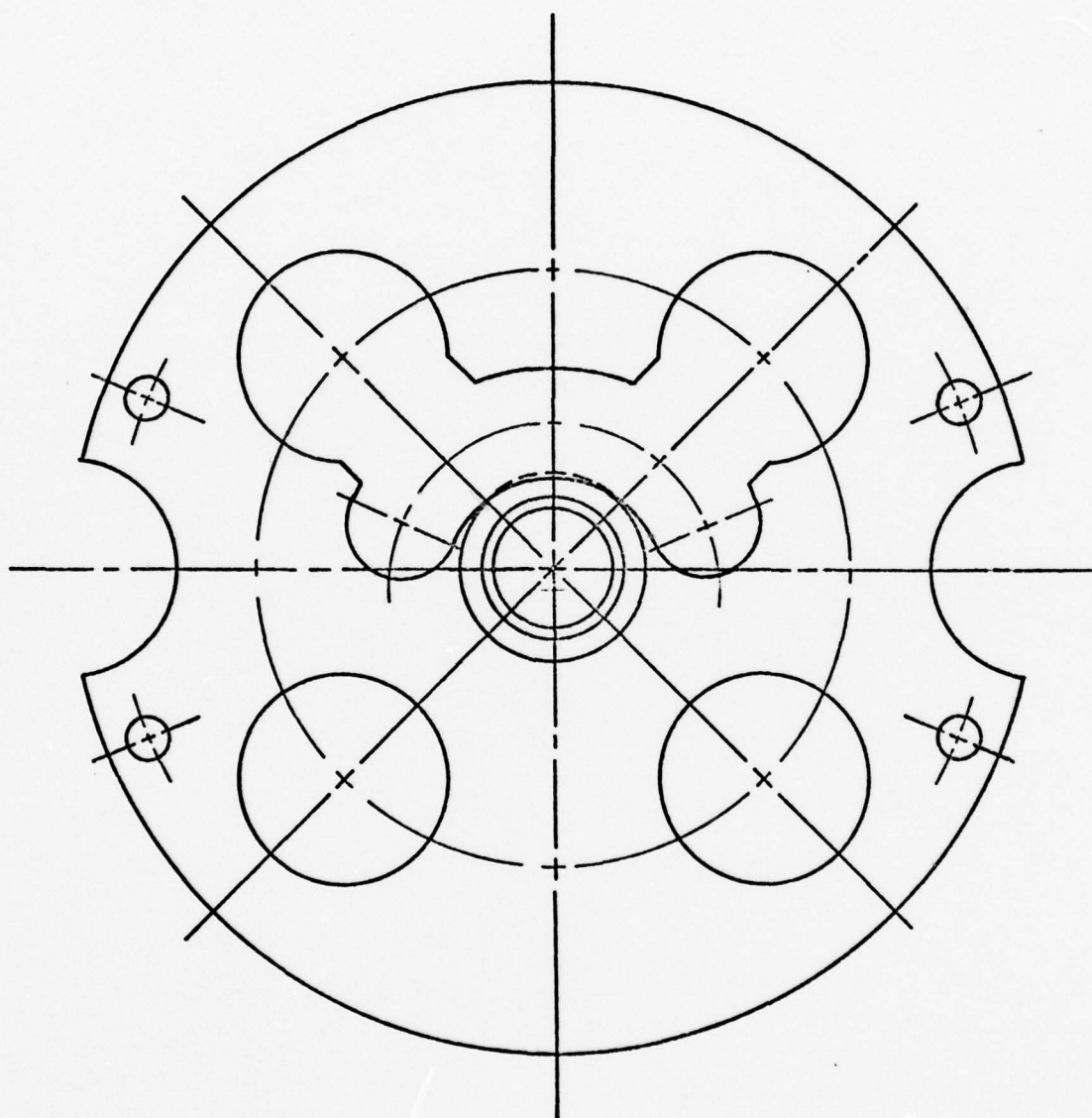
LOSS LINE POLE PIECE CONSTRUCTION

FIG. 7

LOSS

ALUMINA

FIG. 8A

HIGH "Q" LOSS LINE CONSTRUCTION
(UPPER CUTOFF)

LOSS

ALUMINA

FIG. 8B

LOW "Q" LOSS LINE CONSTRUCTION
(IN-BAND)

to achieve the desired effect. The angular orientation
of the stripe with respect to the coupling iris produces
a variable "Q" useful in final cold test determination
of the upper band rolloff characteristic. Figure 9
shows the match and insertion loss characteristics for
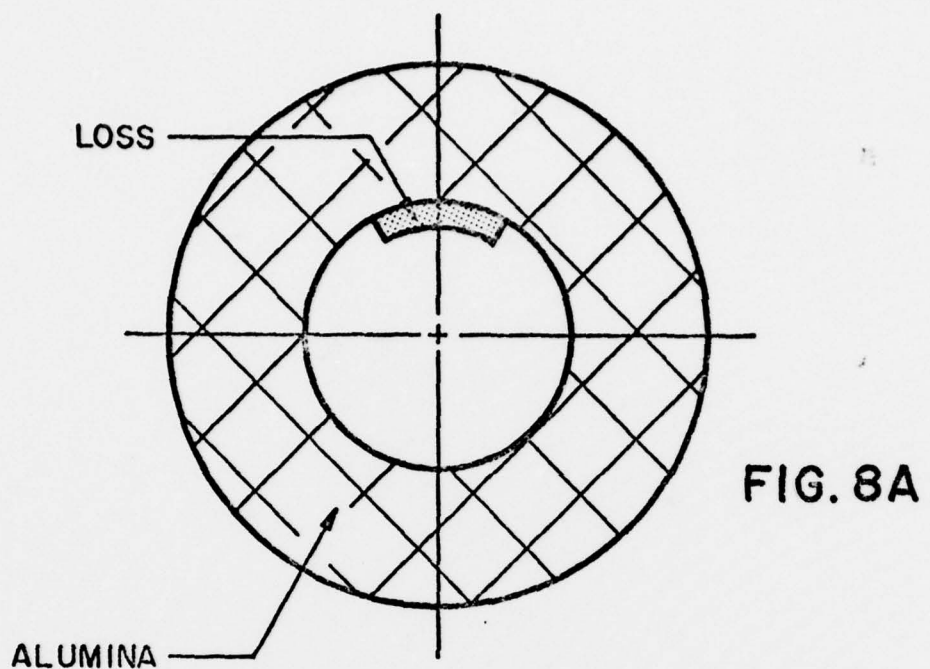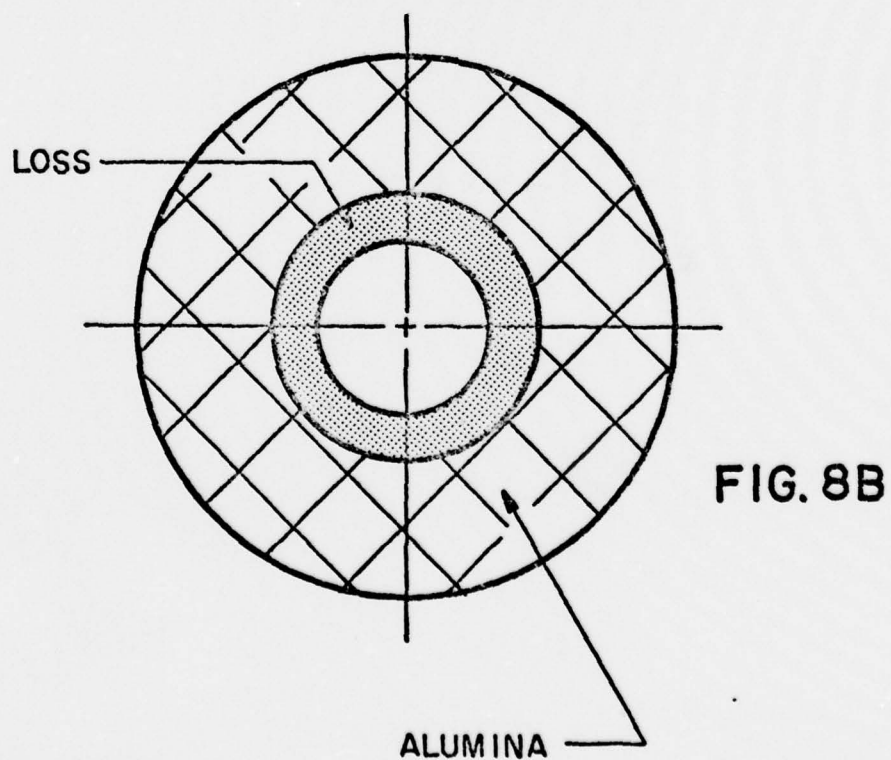S/N 2001. Note the sharp rolloff at the high end of
the band (11 GHz) produced by the "stripers".

A low "Q" construction is achieved with a heavy coating
over the entire inside diameter. The electrical response
is shown at the low end of the band in Figure 9.1. The
resonance is tuned below 7 GHz and the loss "spills" out
over the operating band being very heavy at 7 GHz and
decreasing across the band.

3.3   Cavity Distribution

The cavity distribution for both tubes is shown in
Figure 10. There are 20 cavities in the input section
and 26 cavities in the output section. The input section
has an 8 cavity launch subsection and a 12 cavity attenu-
ator subsection. The output section has a 14 cavity
attenuator subsection, a 4 cavity taper subsection, and
an 8 cavity power subsection. The taper subsection is
an attenuator section with high "Q" in-band loss which
effectively reduces the gain in the 7 - 8 GHz frequency
region but adds very little loss above 9 GHz. This
effectively extends the power section to 12 cavities at
the higher frequencies.

There are 8 loss rods utilized in this tube design, 4 in
each section. Cavities[2] 21, 24, and 49 are manifold
cavities used to convey the fluid to and from the loss
rods. The sever is a standard design. In the early
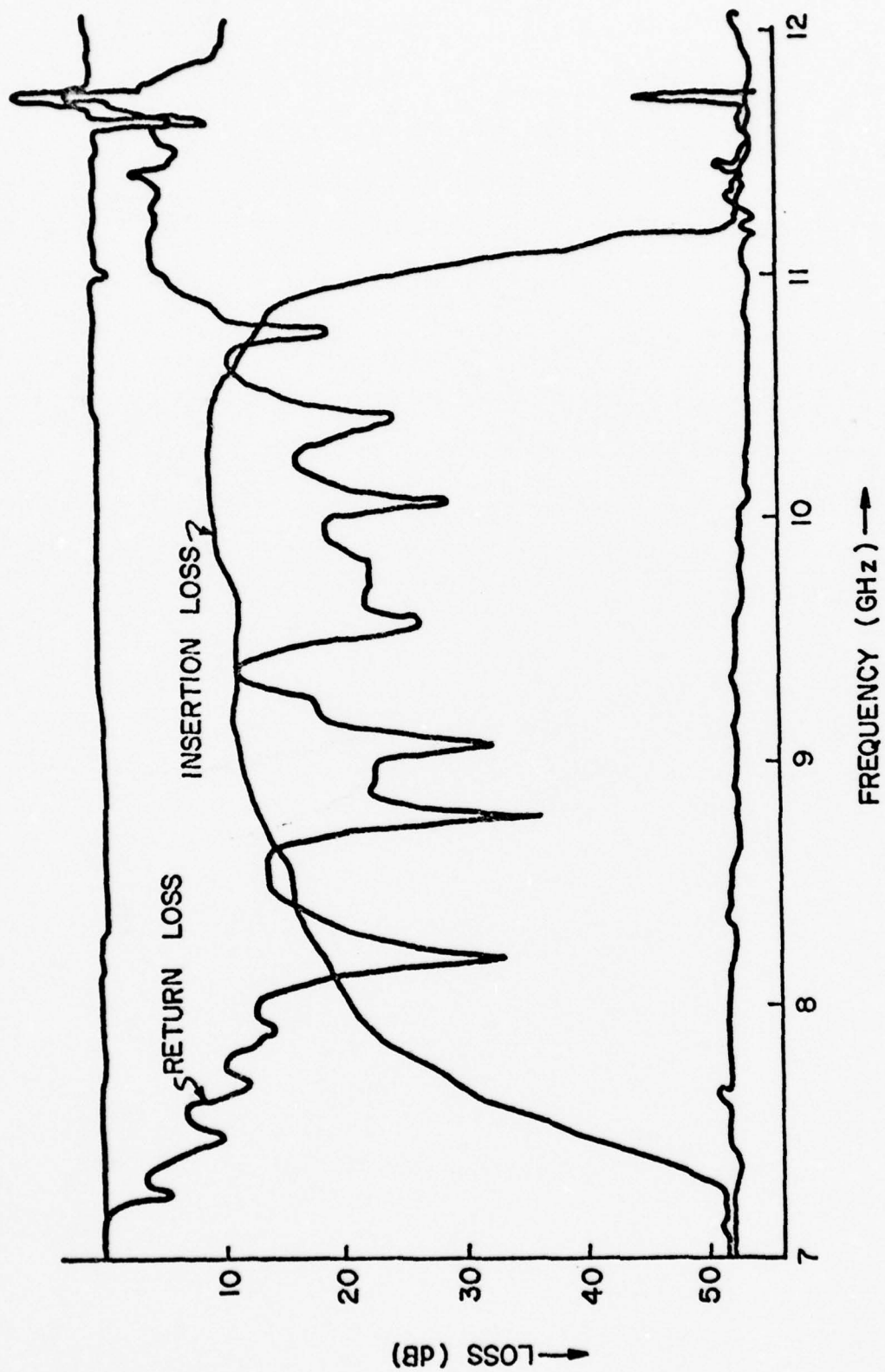
RETURN LOSS AND INSERTION LOSS FOR
THE OUTPUT SECTION OF L-5631, S/N 2001.

FIG.9
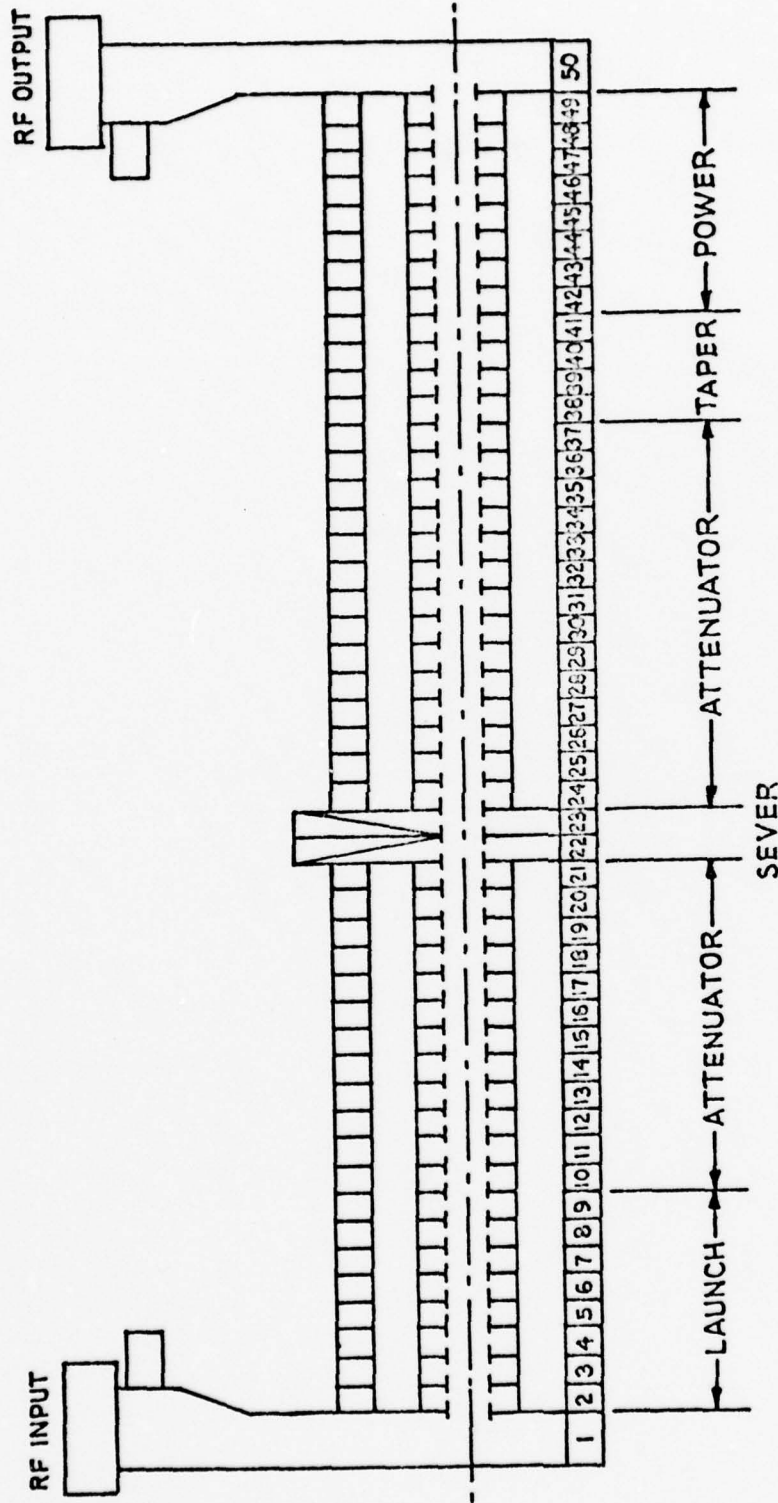
CAVITY DISTRIBUTION

FIG. 10

models of the loss line tube the loss rods extended
the full length of the tube and passed through the
sever. The construction utilized in this design provides
considerably more RF isolation between circuit sections.

Each section, therefore, is complete with its own
set of loss rods. The loss rod assemblies are
shorter and mechanically more stable.

4.0   DESIGN FOR S/N 2001

Figure 11 shows the cavity and loss distribution chart
for S/N 2001. There were 2 symmetric loss lines, Type A,
having .6 dB reference loss and 2 symmetric loss lines,
Type B, having 6 dB reference loss in both the input and
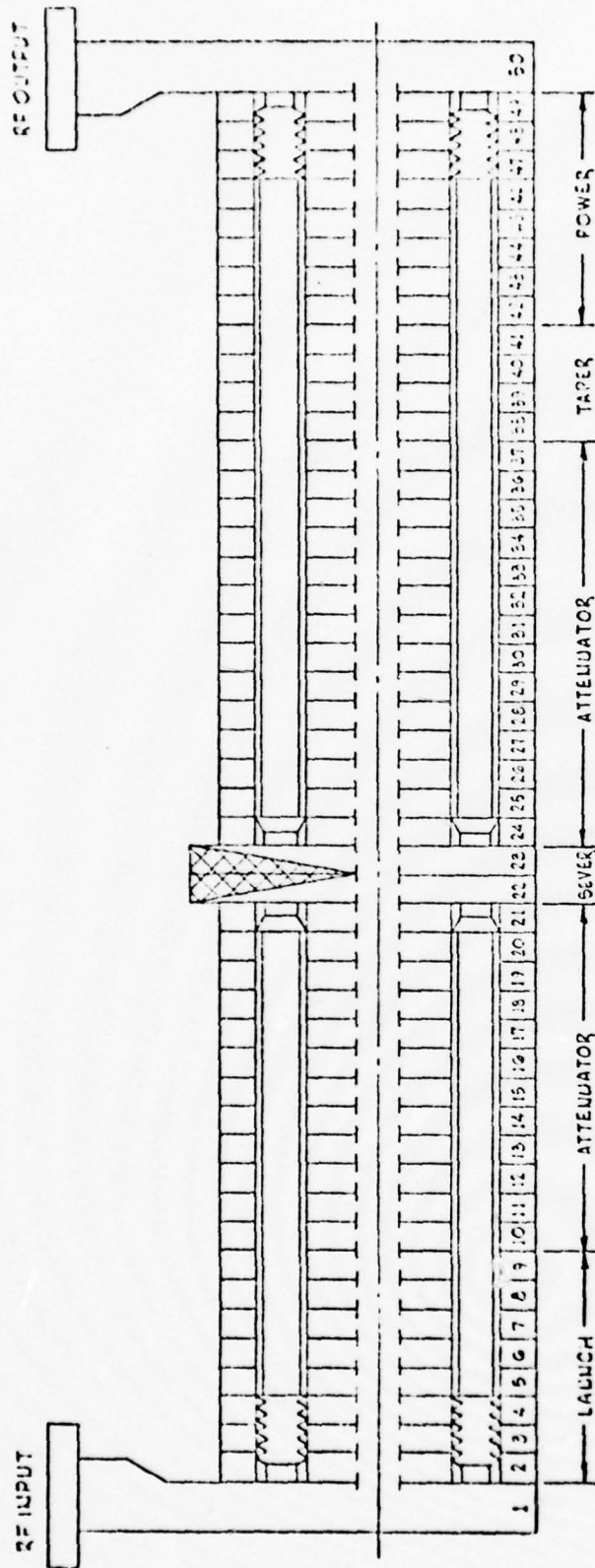output sections. This reference loss or type of loss
is constant over the total length of a specific loss line.

In subsection 1, the launch section, the Type A sleeves
were shorted over the first 3 cavities and have .260 in.
wide X .125 in. long slots in the last 5 cavities. The
Type B sleeves were shorted over the entire length.
Therefore no in-band loss is added in the launch section
and there is no loss at all in the bellows region (first
3 cavities).

In the input attenuator region, subsection 2, the Type A
sleeves have .260 in. wide X .125 in. long slots for every
cavity. The Type B sleeves had continuous slots .125 in.
wide oriented for heavy attenuation. Subsections 1 and 2
were brazed together with the corresponding sleeves. The
loss rods were inserted and welded to the manifold cavities.
The manifold cavities were then brazed to the section.
Loss line covers were welded in place completing the
section construction.

In subsection 3, the output attenuator section, the sleeve
geometries were similar to subsection 2 except that there
were 13 cavities.

The taper section used the same type sleeves as in sub-
sections 2 and 3 except that the angular orientation of the
slot was varied to lower the resonant frequency and produce
a light attenuator.

- 20 -

FIG. 11 LOSS LINE AND SLEEVE DISTRIBUTION S/N 2001

Subsection 5, the power section, was similar to sub-
section 1 and the same sleeves were used with shorted
ends placed at the output end of the section.

Subsections 3, 4 and 5 were brazed together with the
corresponding sleeves and with the loss lines and
manifold cavities in place formed the output section.

Computer runs were made at 7.5 GHz, 9 GHz and 10.5 GHz
for this design. The results of the large signal computer
run at 7.5 GHz are shown in Figure 12. In the launch
section the gain rate is very high but is then sharply
reduced in the attenuator region so that the net gain
is about 24 dB at the sever. After the sever the gain
rate is still curtailed by the attenuator. Even in the
power section the gain rate does not increase until the
last 8 cavities. The tube saturates at about 20 kW and
56 dB large signal gain. The drive characteristics are
shown in Figure 13. AM-PM at saturation is about 1.3°/dB
as calculated from the 12 disk model.

The computer results at midband (9 GHz) are shown in
Figure 14. The effect of the attenuator is smaller at
9 GHz. The gain rate is almost constant throughout the
tube. The tube saturates at about 22 kW and a large
signal gain of about 49 dB. The calculated AM-PM charac-
teristics are shown in Figure 15. At saturation the
calculations show 1°/dB.

In Figure 16 the computer results at 10.5 GHz are shown.
The gain rate is low and some power is transferred outside
the power section indicating that it is not quite long
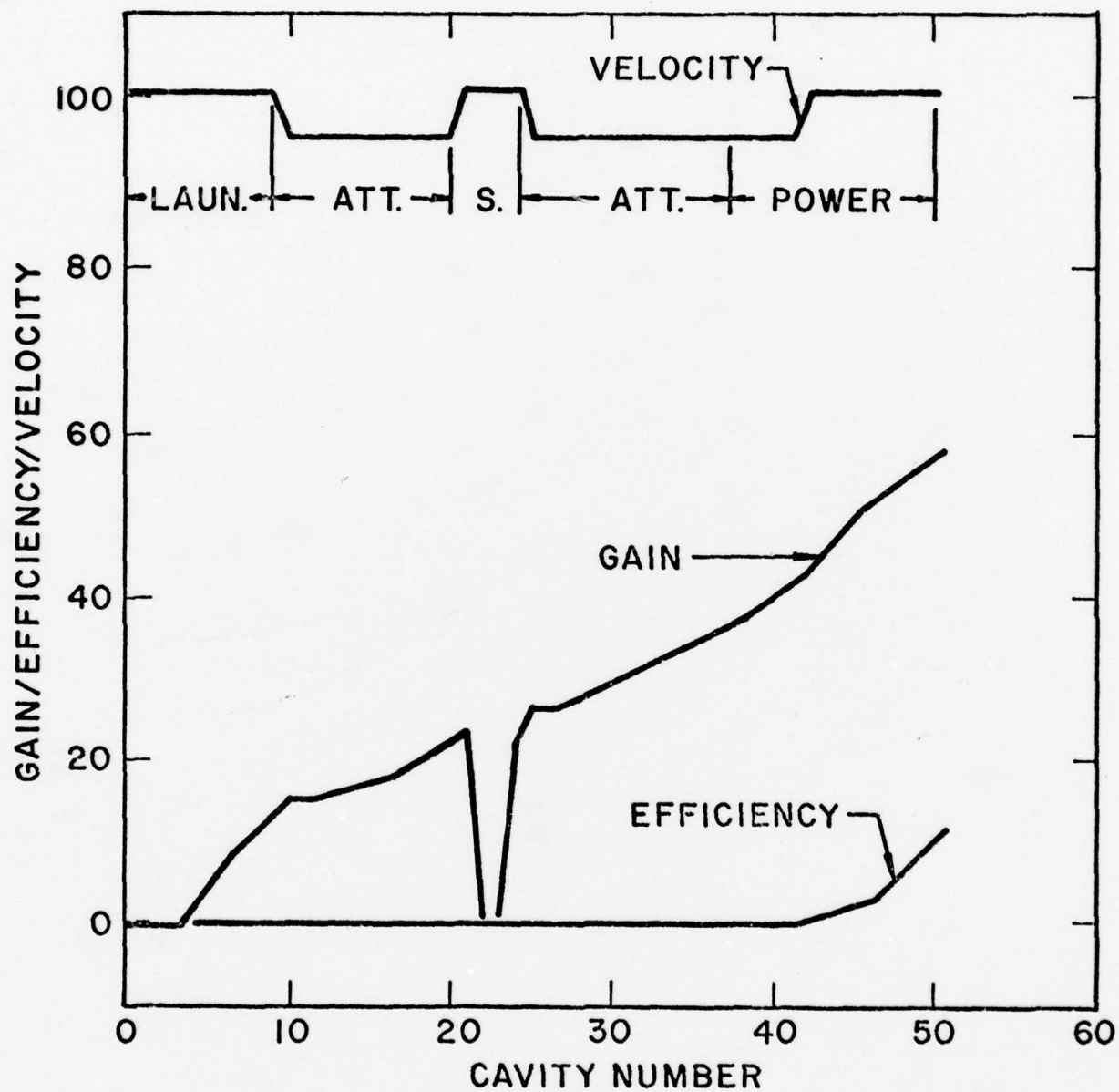
FIG.12   COMPUTER RUN AT 7.5 GHz
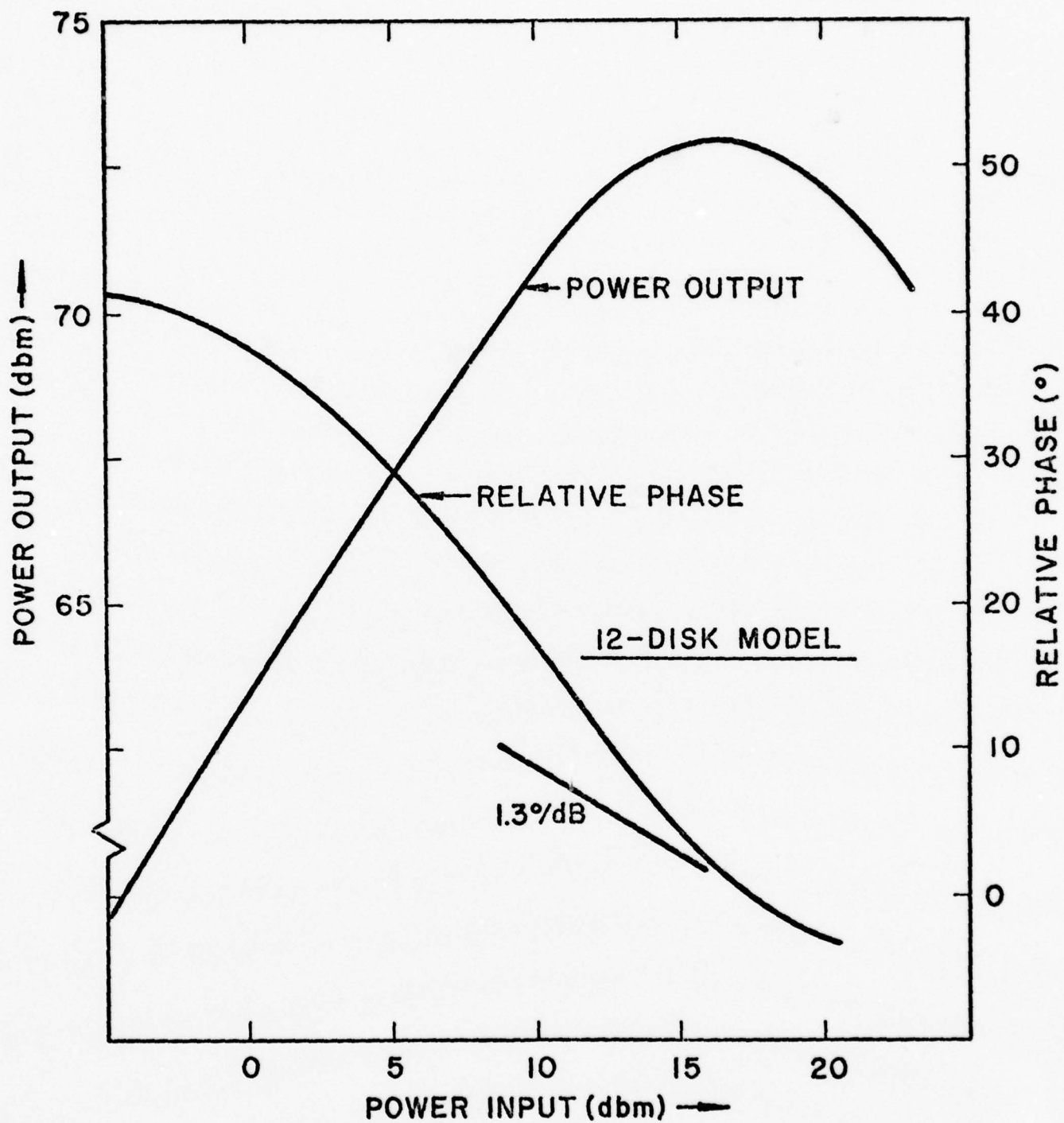
**POWER OUTPUT VS. POWER INPUT
RELATIVE PHASE VS. POWER INPUT
(LOWER BANDEDGE)
FIG. 13**

FIG. 14 COMPUTER RUN AT 9 GHz

POWER OUTPUT VS. POWER INPUT
RELATIVE PHASE VS. POWER INPUT
(MIDBAND)

FIG. 15
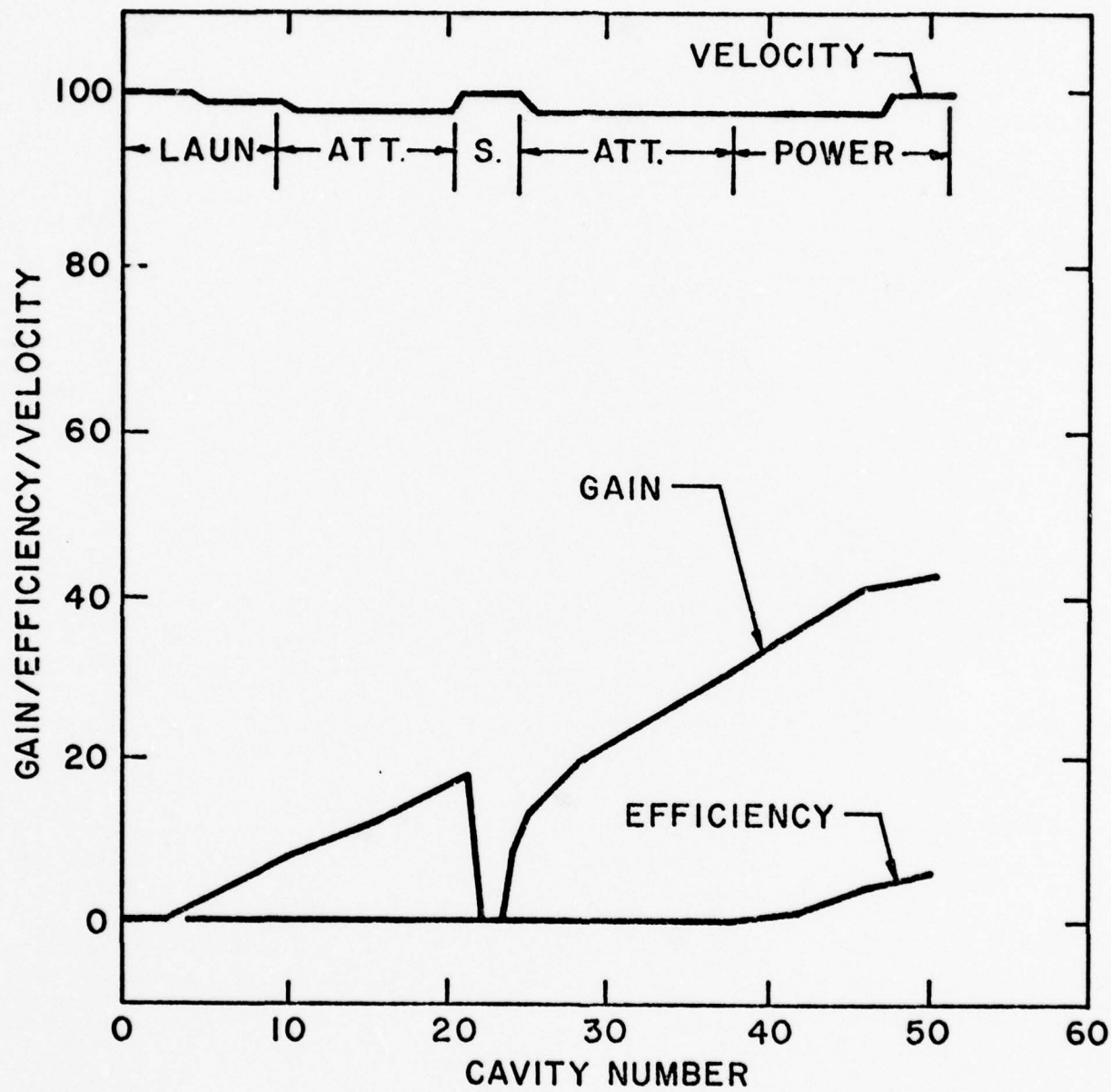
FIG.16 COMPUTER RUN AT 10.5GHz

enough. The calculated output power is 16 kW and
the gain is about 41 dB. The AM-PM characteristics
are shown in Figure 17. At saturation the calculated
AM-PM is about 1.2°/dB.
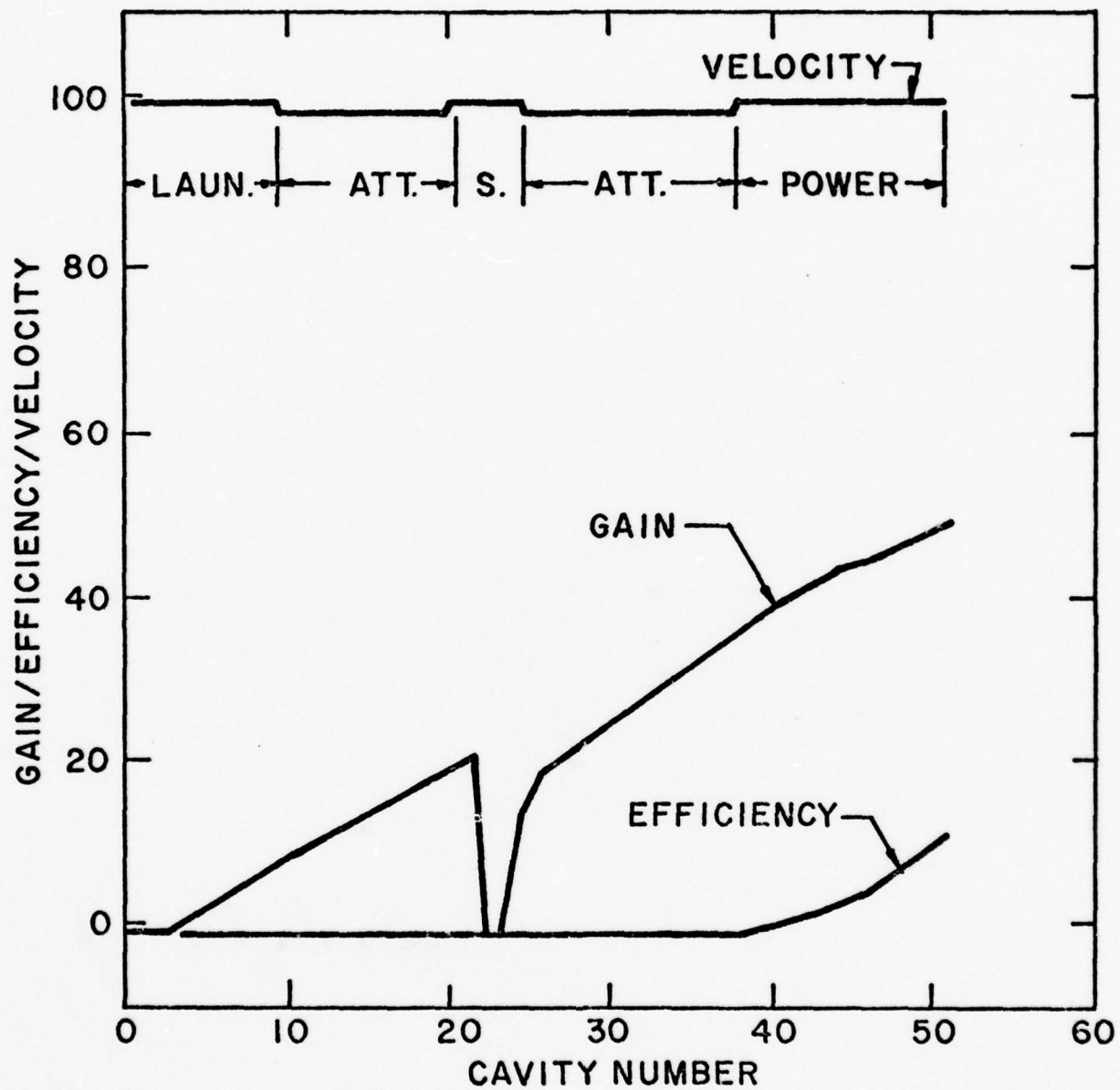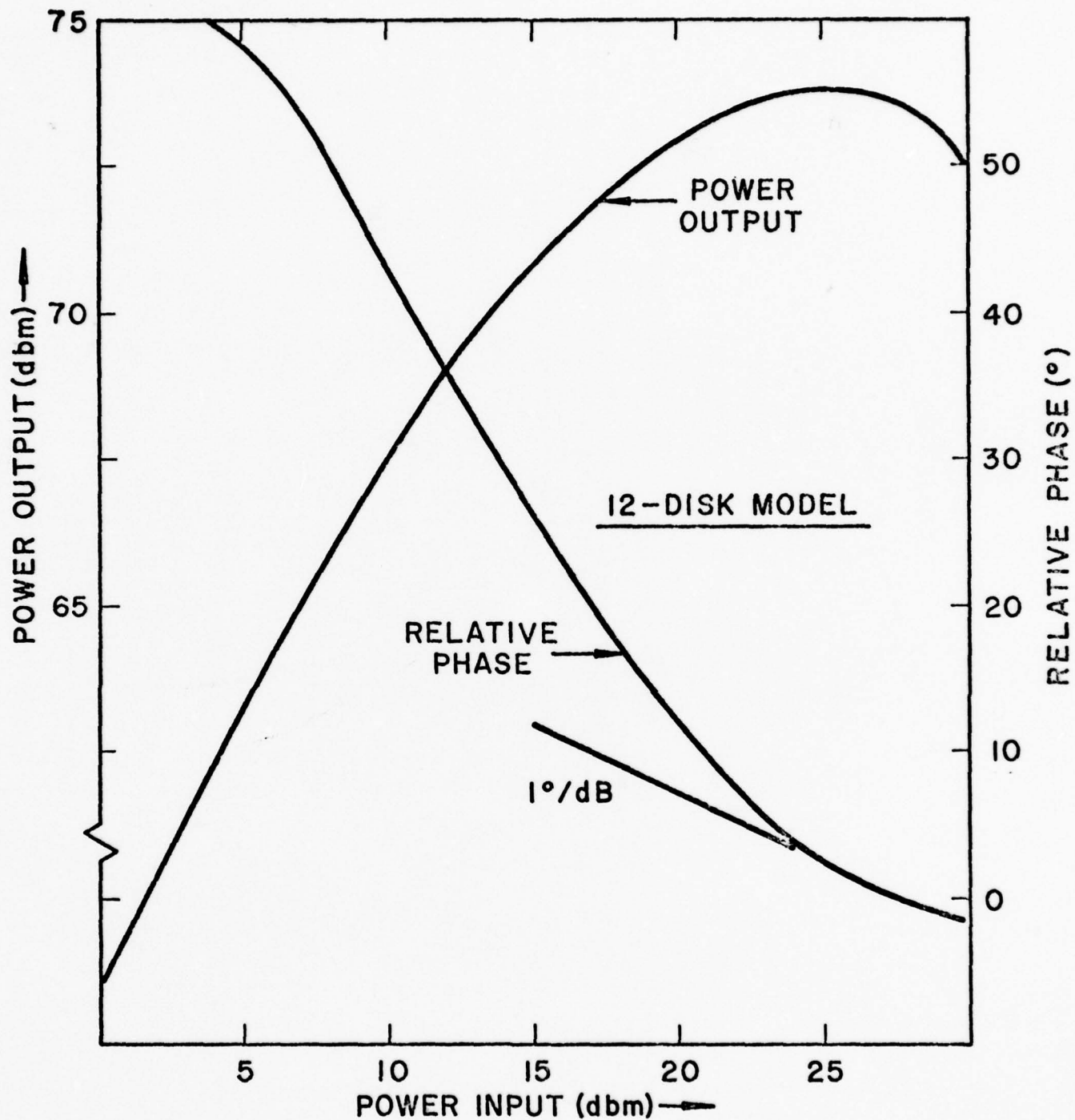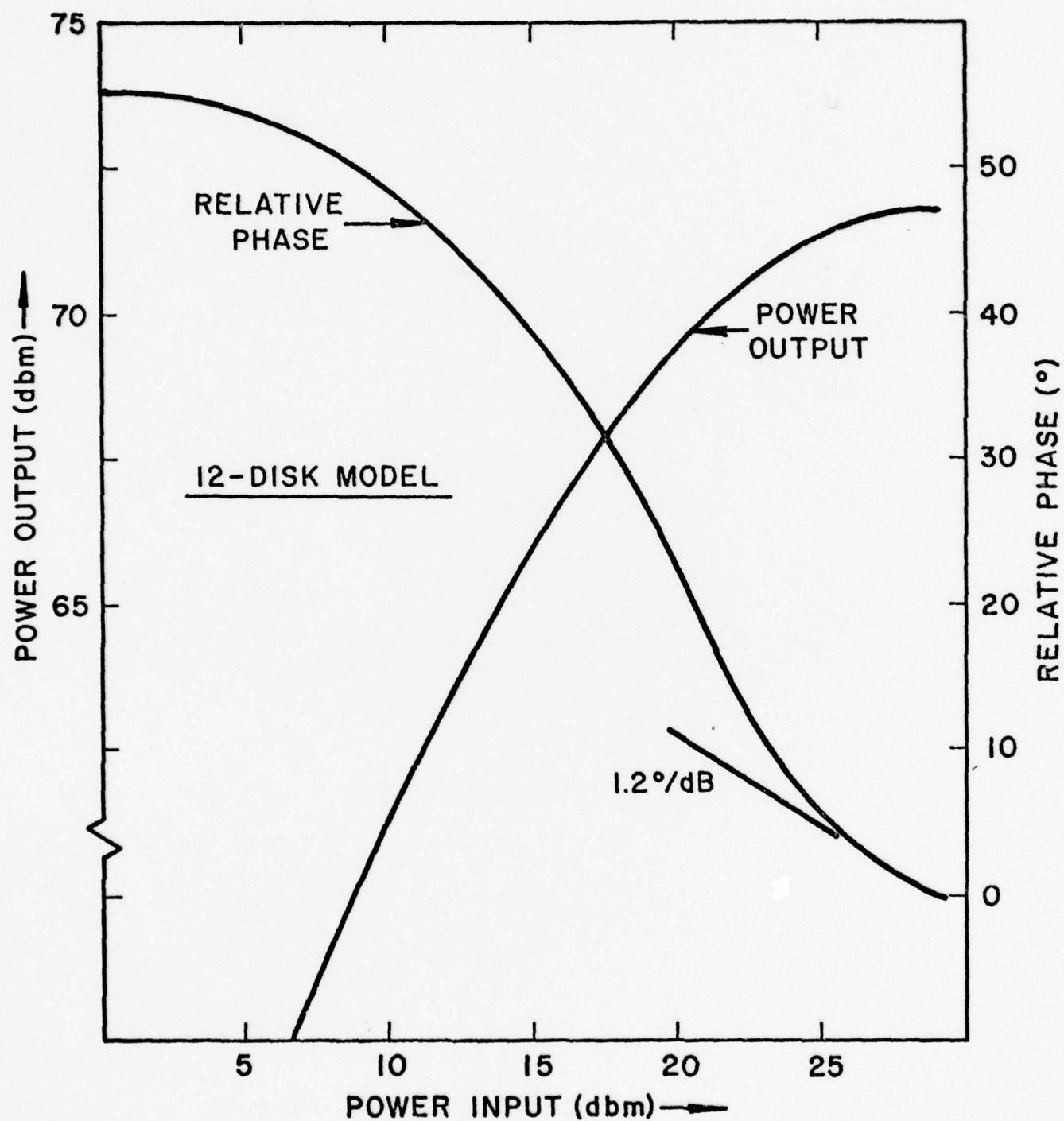
POWER OUTPUT VS. POWER INPUT
RELATIVE PHASE VS. POWER INPUT
(UPPER BANDEDGE)
FIG. 17

5.0 TEST RESULTS FOR S/N 2001

S/N 2001 was focused without RF at .1% duty factor. The initial transmission w/o RF was 92%. Figure 18 shows the RF performance at 32.5 kV, 6A with FC-77 in all the loss lines. The peak output power is greater than 20 kW from 7.4 GHz to 10.85 GHz. From 7.0 GHz to 11.0 GHz the peak output power was greater than 13 kW.

Figure 19 shows the small signal gain variation from 7.0 to 11.0 GHz at 31.5 kV, 32.5 kV and 33.5 kV. At 31.5 kV the gain variation is about 24 dB. At 32.5 kV corresponding to the data in Figure 18 the gain variation is about 35 dB. Note also that at 11 GHz the small signal gain is about 45 dB at 31.5; it is 35 dB at 32.5; and 25 at 33.5 kV. The sensitivity of the tube at 11 GHz is due to the high value of QC and the loss profile in the neighborhood of 11 GHz. Figure 20 shows the output power at 33.5 kV. Note the power falls off rapidly beyond 10.0 GHz.

Raising the cathode voltage and current has the results shown in Figure 21. At 33.5 kV and 7A the tube meets the minimum power specification at the bandedges. The peak power is in excess of 40 kW over most of the band. The transmission for these conditions is about 92.0% without RF. Figure 22 shows the corresponding gain variation over the band is about 40 dB. Note that the minimum small signal gain is 42 dB.

The tube showed no in-band oscillations even at 8A where the small signal gain was clearly in excess of 80 dB.
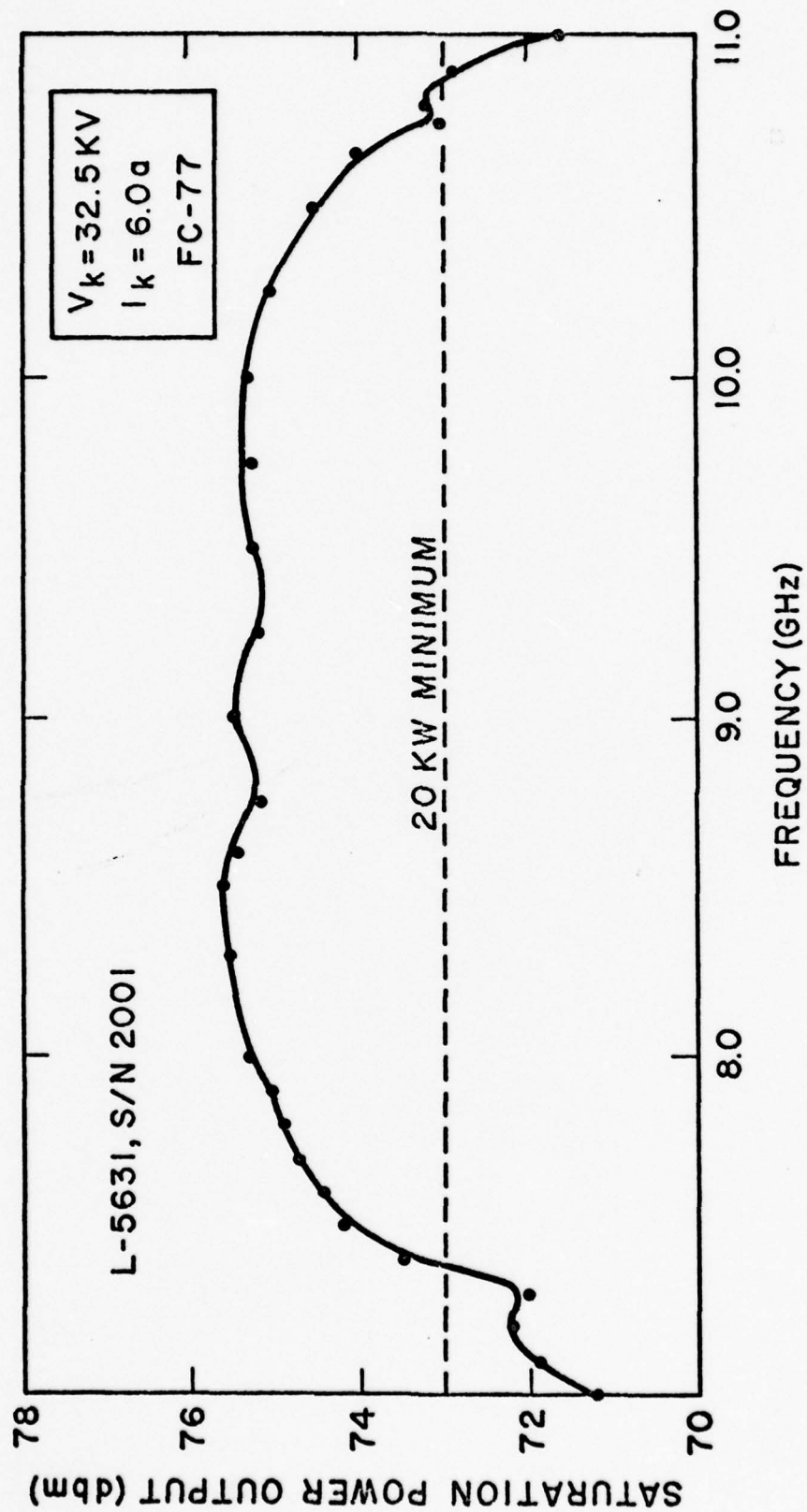
SATURATION POWER OUTPUT VS. FREQUENCY

FIG. 18
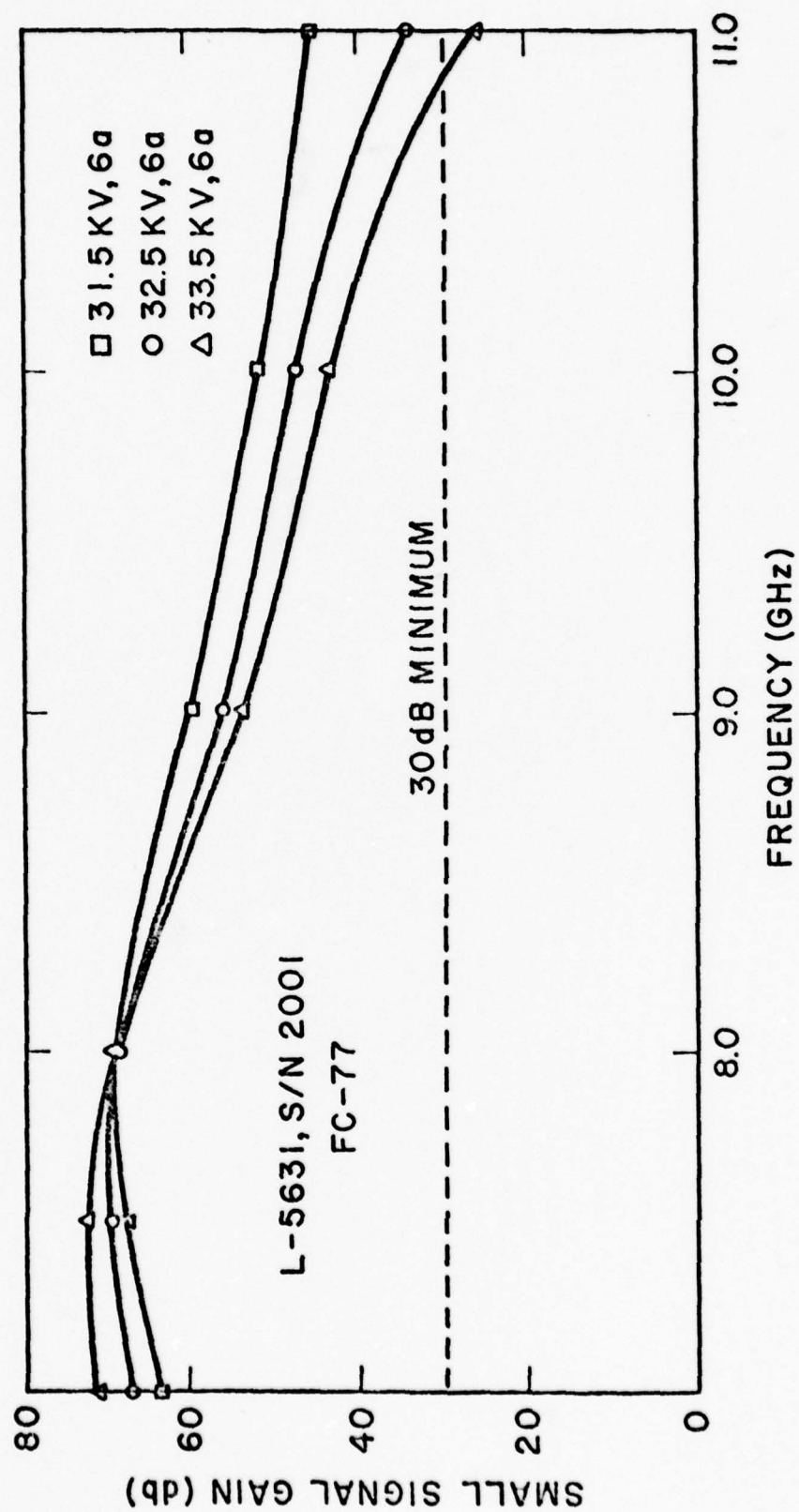
SMALL SIGNAL GAIN VS. FREQUENCY

FIG.19
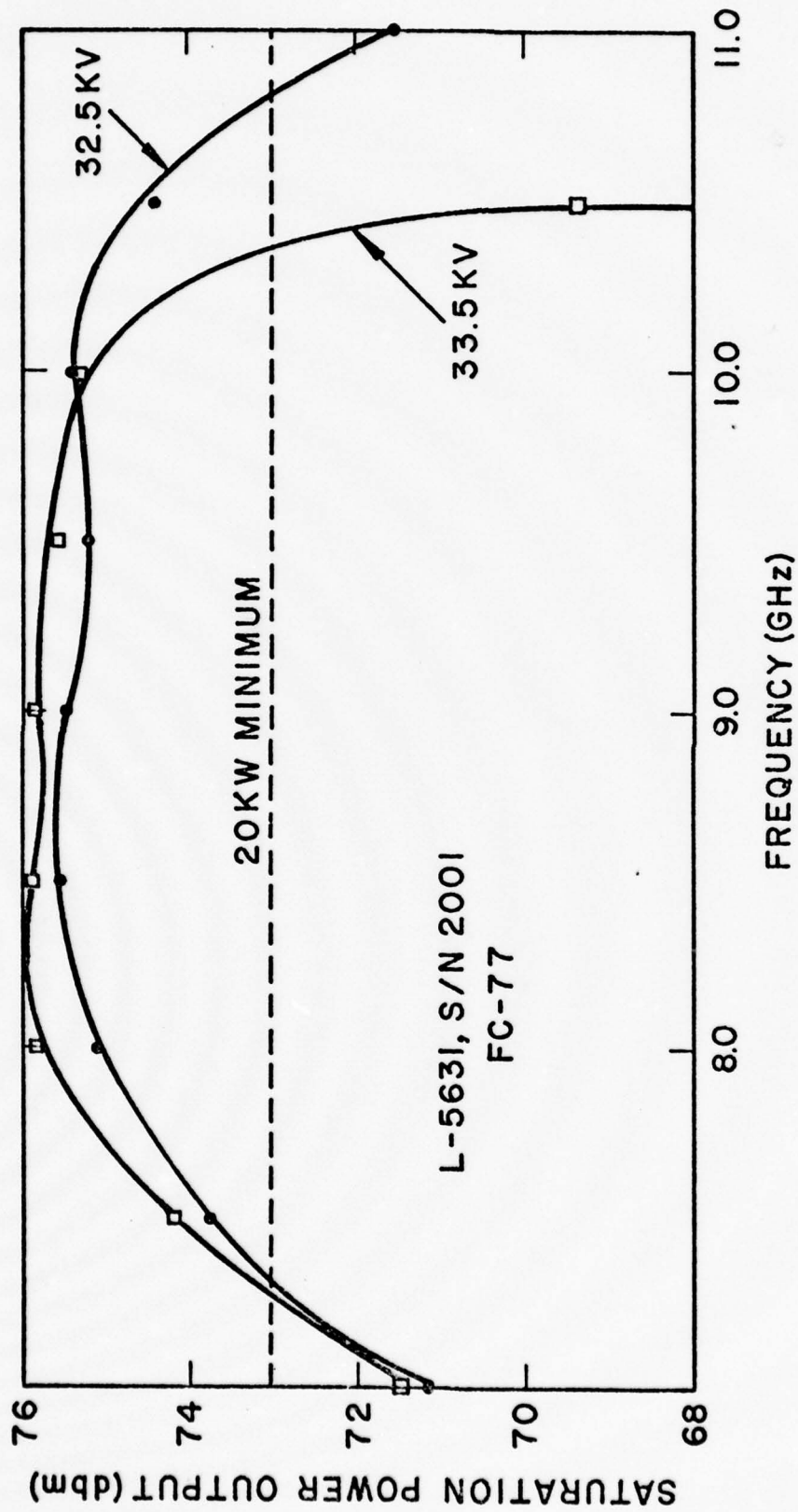
SATURATION POWER OUTPUT VS. FREQUENCY

FIG.20
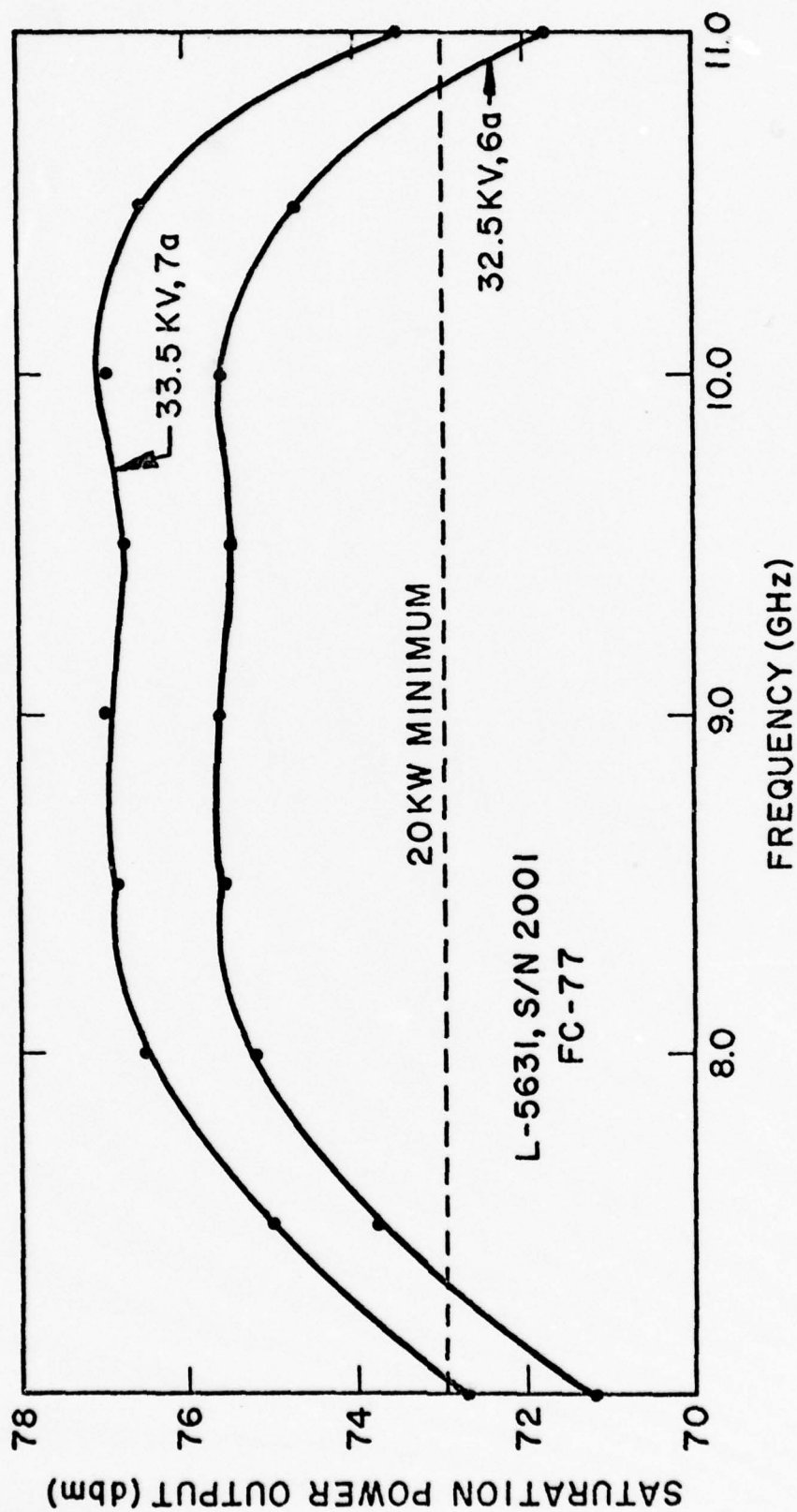
SATURATION POWER OUTPUT VS. FREQUENCY

FIG. 21
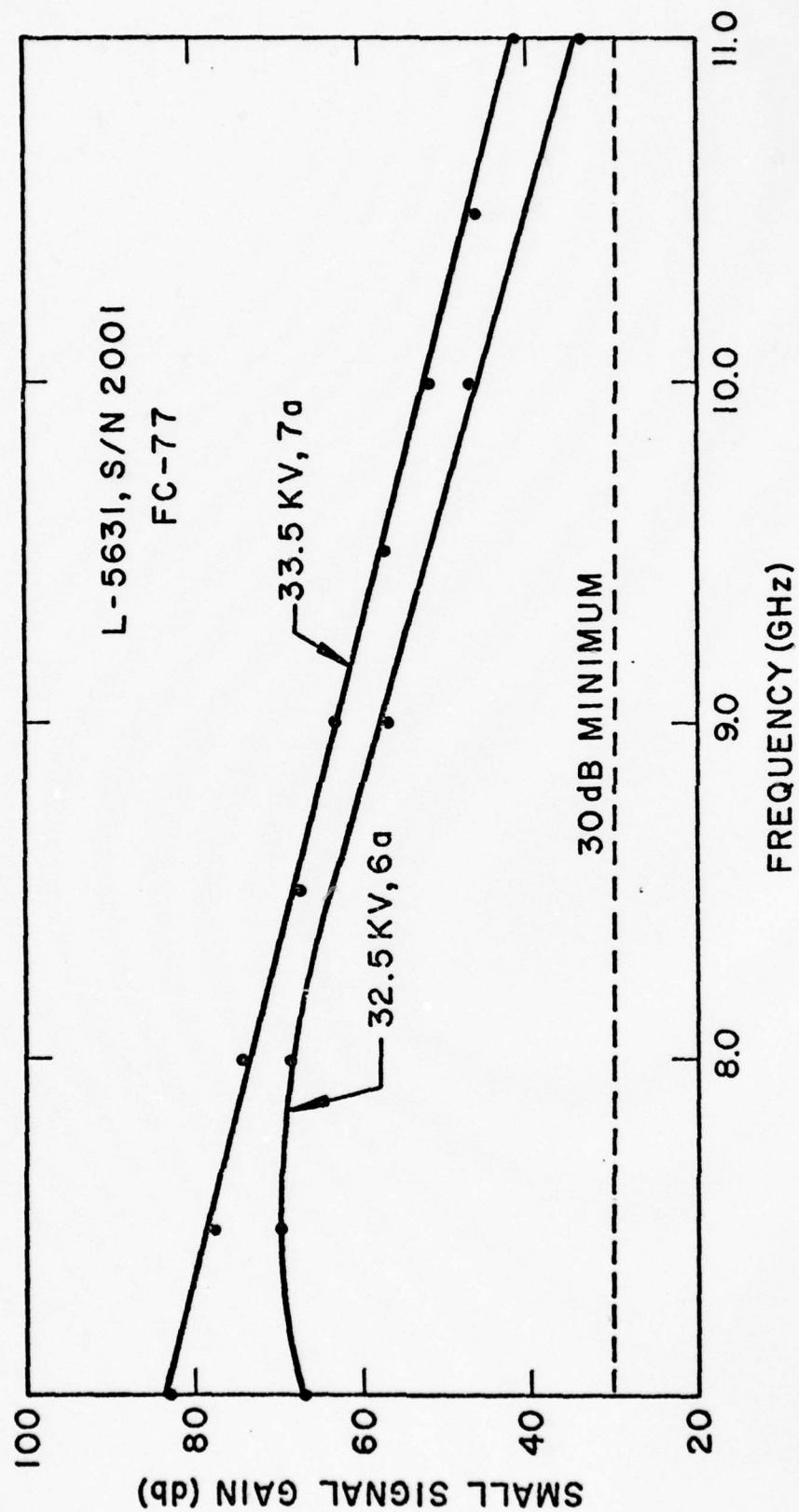
SMALL SIGNAL GAIN VS. FREQUENCY

FIG. 22

The cathode voltage could not be reduced much beyond
32.5 kV with FC-77 in the loss lines without encountering
drive induced oscillations. The tube, however, was
quite stable without drive down to about 31 kV at 6.0A.

In order to operate the tube at cathode voltages less
than 32.5 kV different fluids were used in the loss
lines. The results with ethyl alcohol are shown in
Figure 23. The tube was quite stable with drive at lower
cathode voltages but the performance was poor due to the
high loss tangent of ethyl alcohol. Comparison with the
performance of FC-77 at 32.5 kV, 6A shows that increased
loss extended well into the operating band.

A suitable coolant having a low loss tangent and a
slightly higher dielectric constant than FC-77 is DC-200.
This fluid is currently used in Litton carcinotrons.
Figure 24 shows data with DC-200 compared to FC-77.
Notice that the power is lower at 11.0. Approximately
150 MHz of band has been lost for the same power output;
that is, at 10.85 GHz the same power output is obtained
as with FC-77 at 11.0 GHz. The tube with DC-200 is com-
pletely free of drive induced oscillations for cathode
voltages as low as 31 kV.

Figure 25 shows the power data for 31.5 kV, 6A. The
power is lower across the band and particularly at 7.0 GHz
where it is about 1 dB lower. At 11 GHz the power is
nearly the same as shown in Figure 24 so that the saturated
power has a more symmetric shape.

The cathode voltage was set at 31.5 kV, 6.5A and AM-PM
data was taken across the band. This data is shown in
Figure 26. The tube was set up at saturation and the

- 36 -
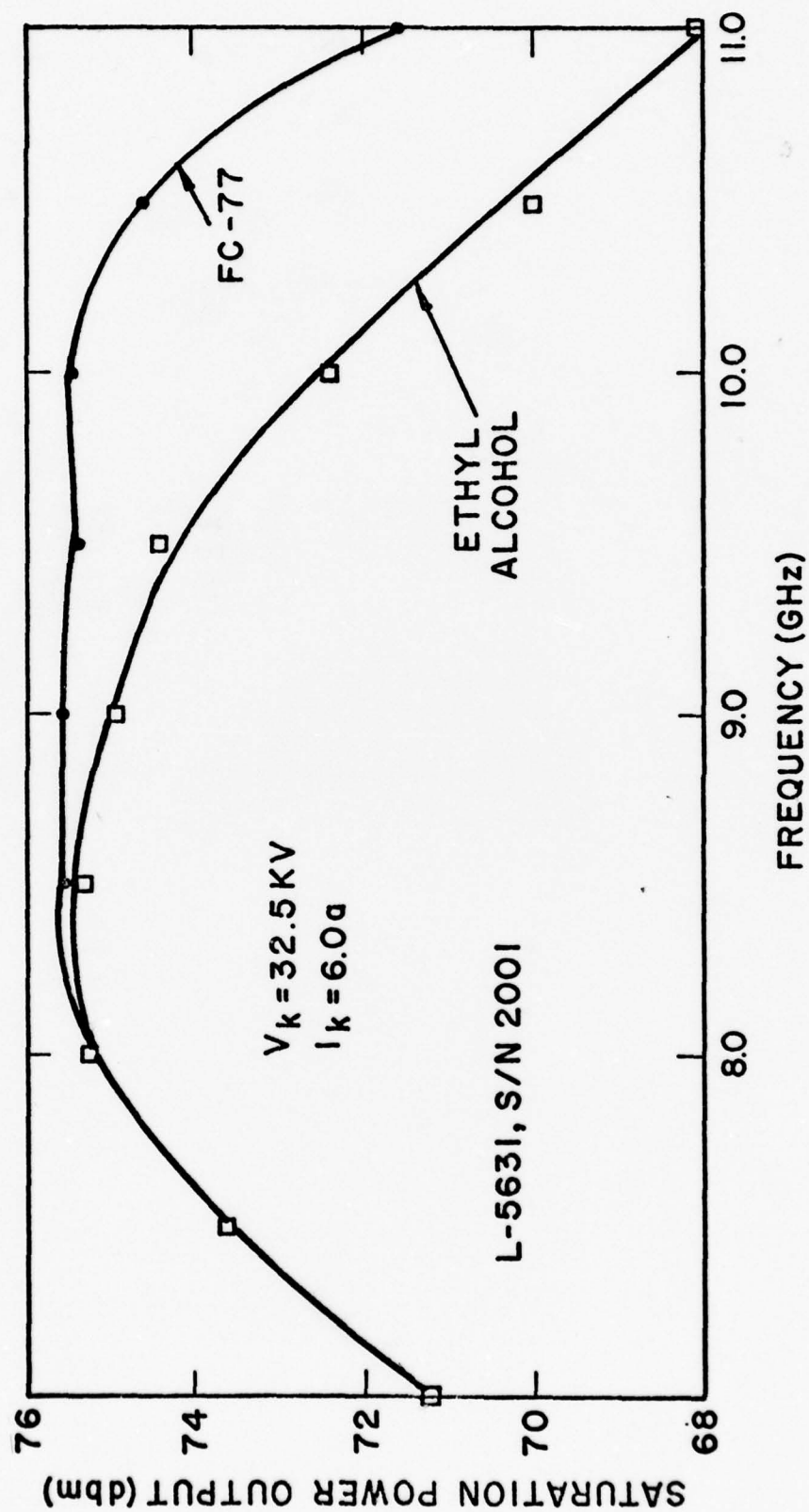
SATURATION POWER OUTPUT VS. FREQUENCY

FIG. 23
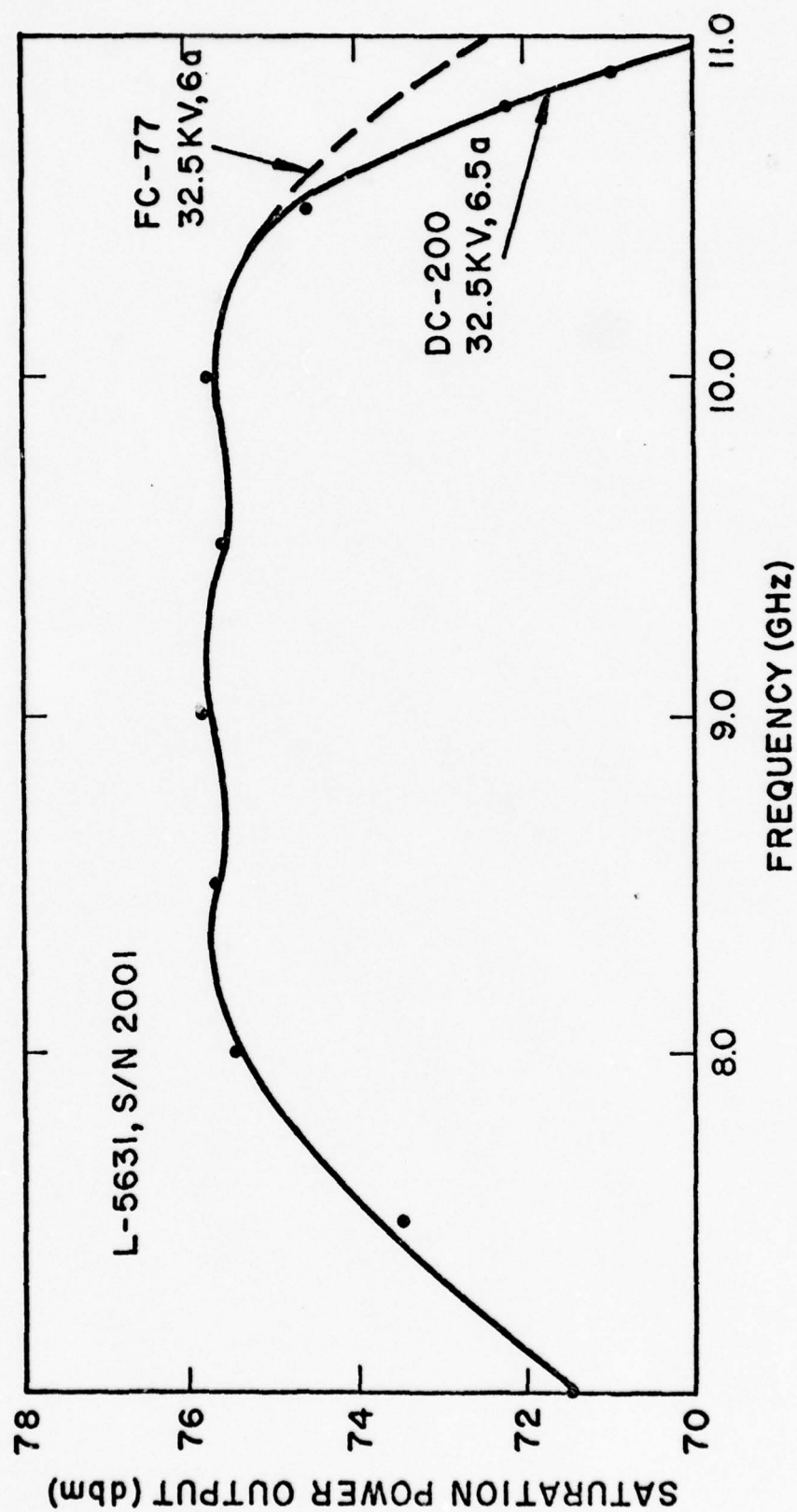
SATURATION POWER OUTPUT VS. FREQUENCY

FIG. 24

- 38 -
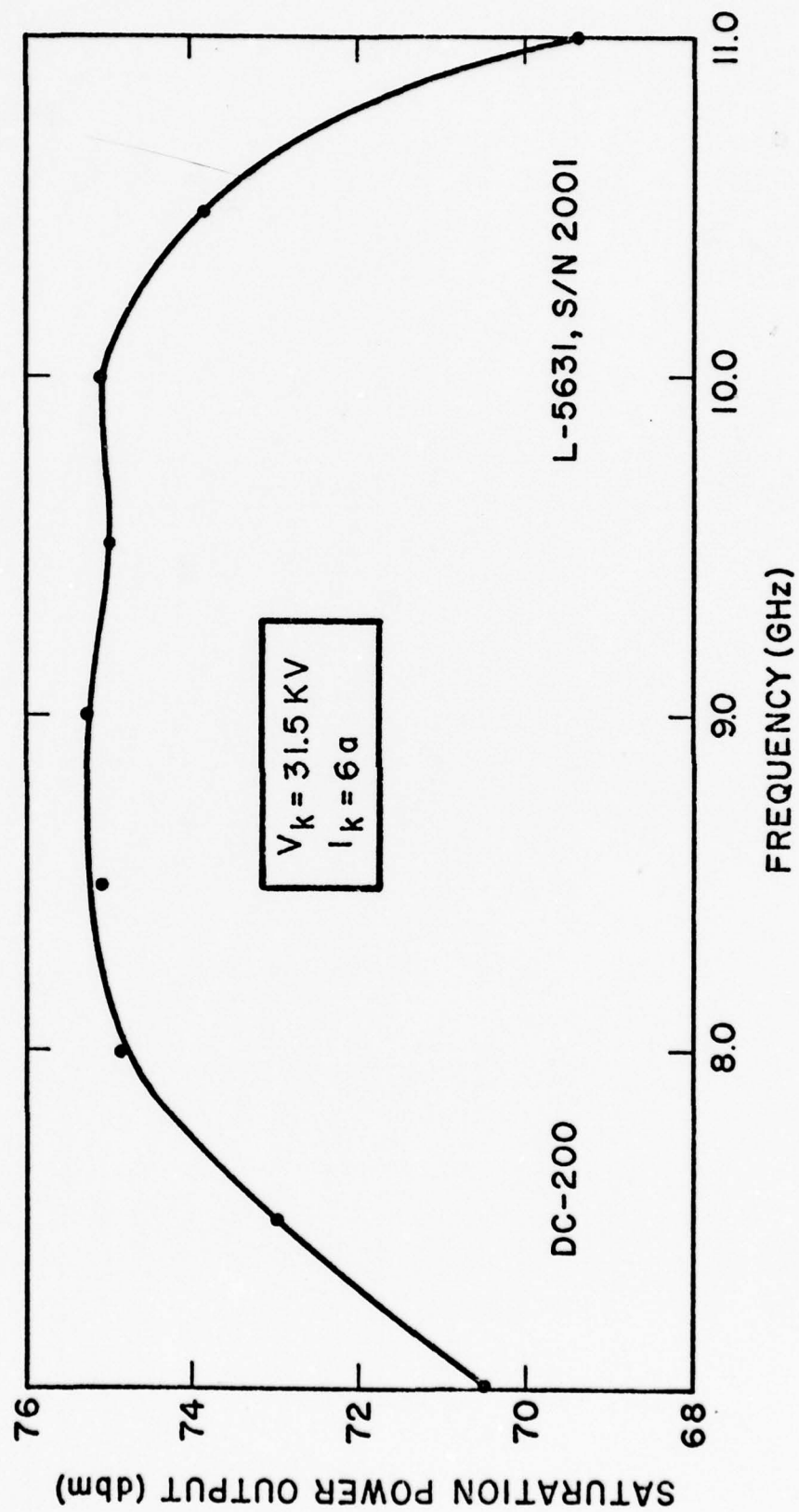
SATURATION POWER OUTPUT VS. FREQUENCY

FIG. 25
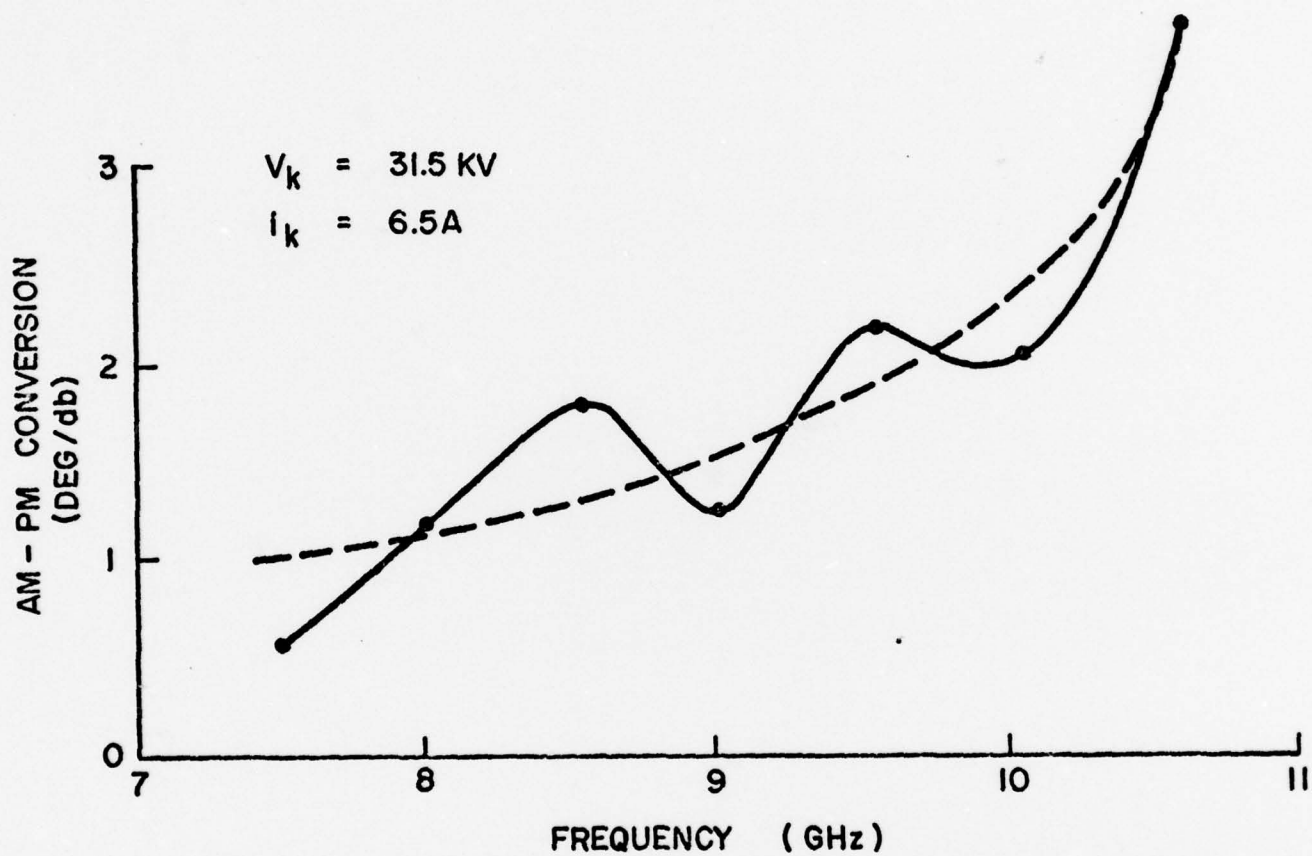
AVERAGE AM-PM OVER
0 TO -10db DYNAMIC
RANGE.

FIG. 26

drive power was reduced 10 dB. The total phase deviation
over the range was divided by 10 to obtain an average
AM-PM number. In the frequency region from 10.0 to 11.0
the phase deviation was large enough to make more refined
measurements. The high value of AM-PM at 11.0 GHz is
due to several factors:

1. The increased dielectric loading at 11.0 causes
    the velocity of the circuit to be lower so
    that the circuit is strongly overvoltaged at this
    frequency.

2. The impedance of the circuit is lowered consid-
    erably, thus the gain is low, the output section
    is too short causing sever effects.

3. The loss per unit length is increased particu-
    larly in the power section which is detrimental
    to AM-PM conversion.

Start oscillation data was taken for the tube and is shown
in Figure 27. Oscillations occurred primarily in the
input section. This was due in part to the higher current
in the section, but mostly due to the poor rolloff at the
high end of the band. With air in the loss lines the start
oscillation current was minimum. The oscillation frequency
varied from about 11.05 to 11.22. With FC-77 the oscillations
had a higher threshold. With DC-200 no oscillations were
observed above 30 kV. The only output section oscillation
occurred near 11.0 GHz when drive was applied to the tube
at particular voltage and current levels which maximized the
gain at about 11.0 GHz.

The tube was final focused with DC-200 at 32.5 kV and 6.5A
for full duty operation. Transmission without RF was 95%. The
tube was run at 2% duty factor. There were no significant
changes in the tube at 2% duty. There was a gradual .2 dB
change in the power at 11.0 GHz from the snap on power value
after about 20 seconds. At 1% duty about .1 dB change was seen.
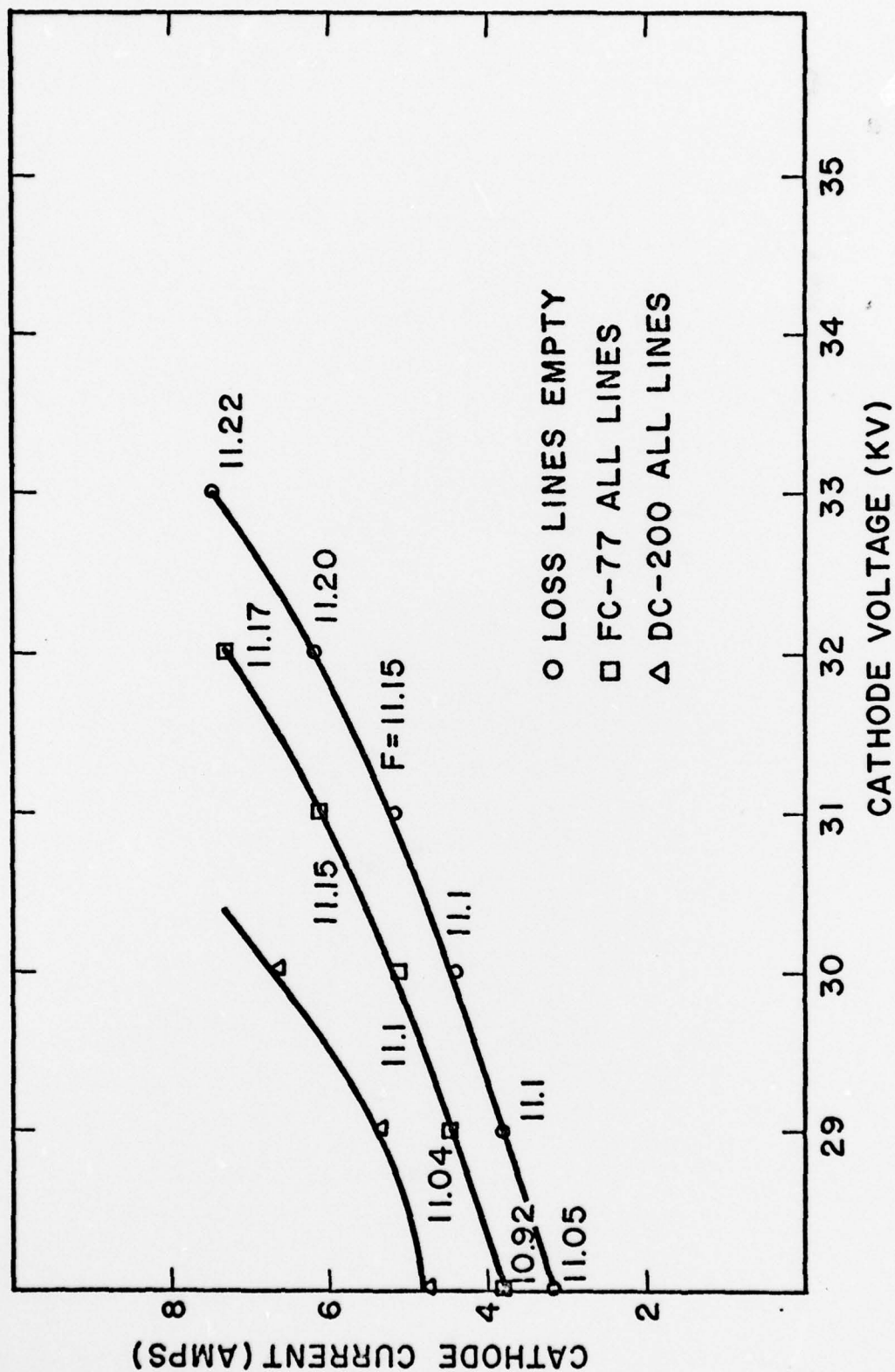
START OSCILLATION DATA (INPUT SECTION)
L-5631 S/N 2001

FIG. 27

6.0 DESIGN FOR S/N 2002

S/N 2002 was built like S/N 2001. With the exception
of the loss-line sleeves all other tube parts were the
same. Figure 28 shows the cavity and loss distribution
chart for S/N 2002 design. The input section consisted
of 20 cavities and the output section of 26 cavities.
This is the same cavity distribution used in S/N 2001.
The output section was composed of three subsections
also as S/N 2001 with approximately the same average
cavity loading. The bellows in the 2002 design has
been placed at the termination end of the section. This
allowed 2 more cavities at the output end to be loaded
with upper cutoff loss. There were four completely un-
loaded cavities in S/N 2001 at the output end whereas in
S/N 2002 there were only 2. This change was made to
eliminate the drive induced oscillations seen in S/N 2001.
This was accomplished as demonstrated in the testing of
the tube (Section 7.0).

RF OUTPUT

RF INPUT

| 1 | 2 | 3 | 4 | 5 | 6 | 7 | 8 | 9 | 10 | 11 | 12 | 13 | 14 | 15 | 16 | 17 | 18 | 19 | 20 | 21 | 22 | 23 | 24 | 25 | 26 | 27 | 28 | 29 | 30 | 31 | 32 | 33 | 34 | 35 | 36 | 37 | 38 | 39 | 40 | 41 | 42 | 43 | 44 | 45 | 46 | 47 | 48 | 49 | 50 |

LAUNCH — ATTENUATOR — SEVER — ATTENUATOR — TAPER — POWER
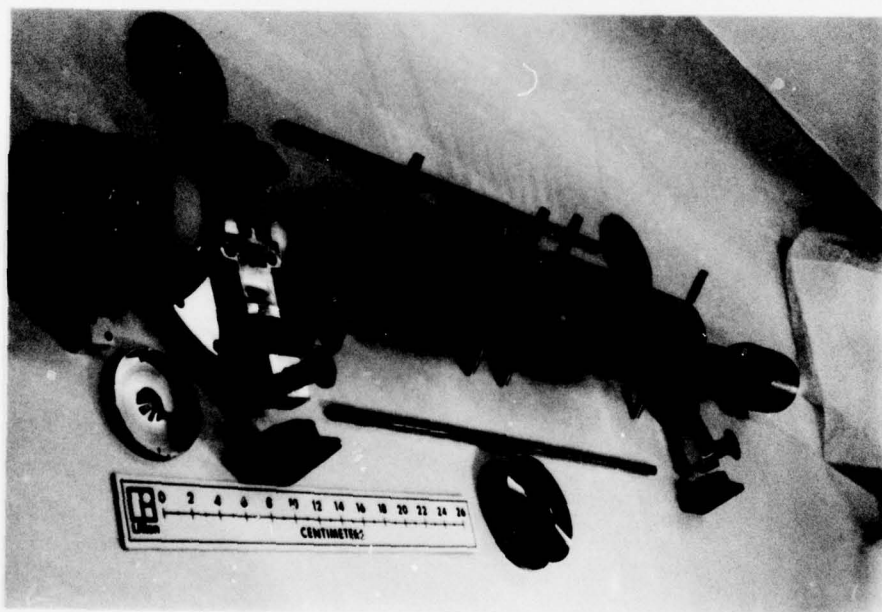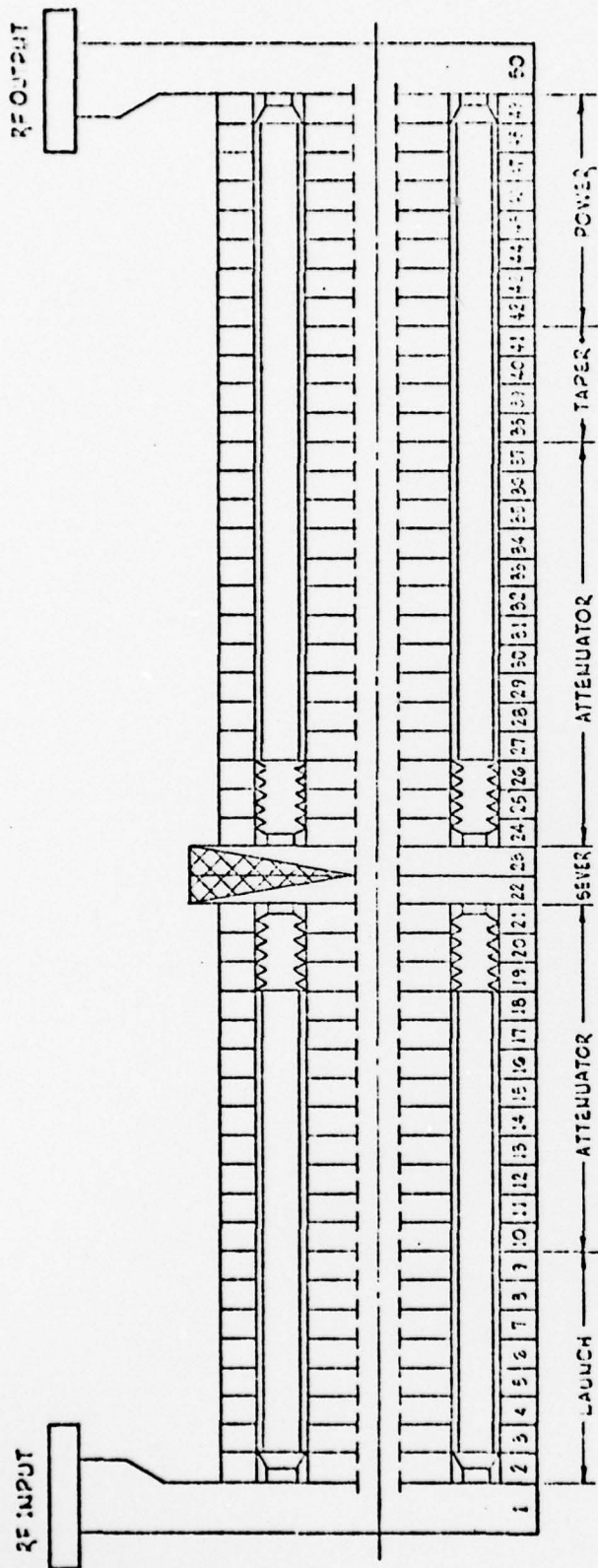
2 SYMMETRICAL (REF=.4/.6dB) LOSS LINE A

SLOT	WIDTH	I/CAV	I/CAVITY (CENTERED)	UN.LD.
WIDTH	.200	.220	.260	SHT.
HEIGHT	.125	.125	.125	SLVS.

2 SYMMETRICAL (REF=.4/.6dB) LOSS LINE A

UN.LD.	I/CAVITY (CENTERED)	I/CAV	WIDTH	I/CAV	SLOT
SHT.	.260	.260	.220	.200	WIDTH
SLVS.	.125	.125	.125	.125	HEIGHT

2 SYMMETRICAL (REF=0/8dB) LOSS LINE B

SLOT	UN-LOADED	HEAVY ATTENUATOR	UN.LD.
WIDTH	SHORTED	CONTINUOUS	SHT.
HEIGHT	SLEEVES	.125	SLVS.

2 SYMMETRICAL (REF=0/8dB) LOSS LINE B

UN.LD.	HEAVY ATTENUATOR	LIGHT	UN-LOADED	SLOT
SHT.	CONTINUOUS	CONT.	SHORTED	WIDTH
SLVS.	.125	.125	SLEEVES	HEIGHT

FIG. 28 LOSS LINE AND SLEEVE DISTRIBUTION S/N 2002

- 44 -

7.0 S/N 2002 TEST RESULTS

S/N 2002 was focused without RF at .1% duty factor.
The transmission was 94% at 32.5 kV, 6.5A.   Figure 29
shows the RF performance with FC-77 in the output loss
lines.   This saturated power performance is very similar
to S/N 2001 as would be expected since the two tubes are
of very similar design.   This tube, S/N 2002, is however
stable with FC-77 and shows no drive induced instabil-
ities. (See Section 6.0).

The output power is greater than 20 kW from 7.5 to 10.7 GHz
with a midband efficiency of greater than 15% with no
collector depression.   The bandedge power at 7.0 GHz and
11 GHz is greater than 10 kW.

Figure 30 shows the large signal gain versus frequency
corresponding to the saturated output power in Figure 29.
The gain maximum of 70 dB occurs at 8.0 GHz.   The minimum
is 36 dB at 11 GHz.

Figure 31 shows the start oscillation data for this tube.
This input section is very stable.   This section can be
undervoltaged down to 29.5 kV at 6.4A without oscillation.
In the unstable zone, the oscillation occurs around a
little dip in the insertion loss.   This dip can be eliminated
by increasing the reference loss slightly in the loss lines,
but is not a serious problem as the data shows.

The output section stability is not as good.   This is
because the output section is longer than the input and
the rolloff is not as sharp.   It is, however, sufficiently
good for a stable tube at 6.5A and 31 kV.
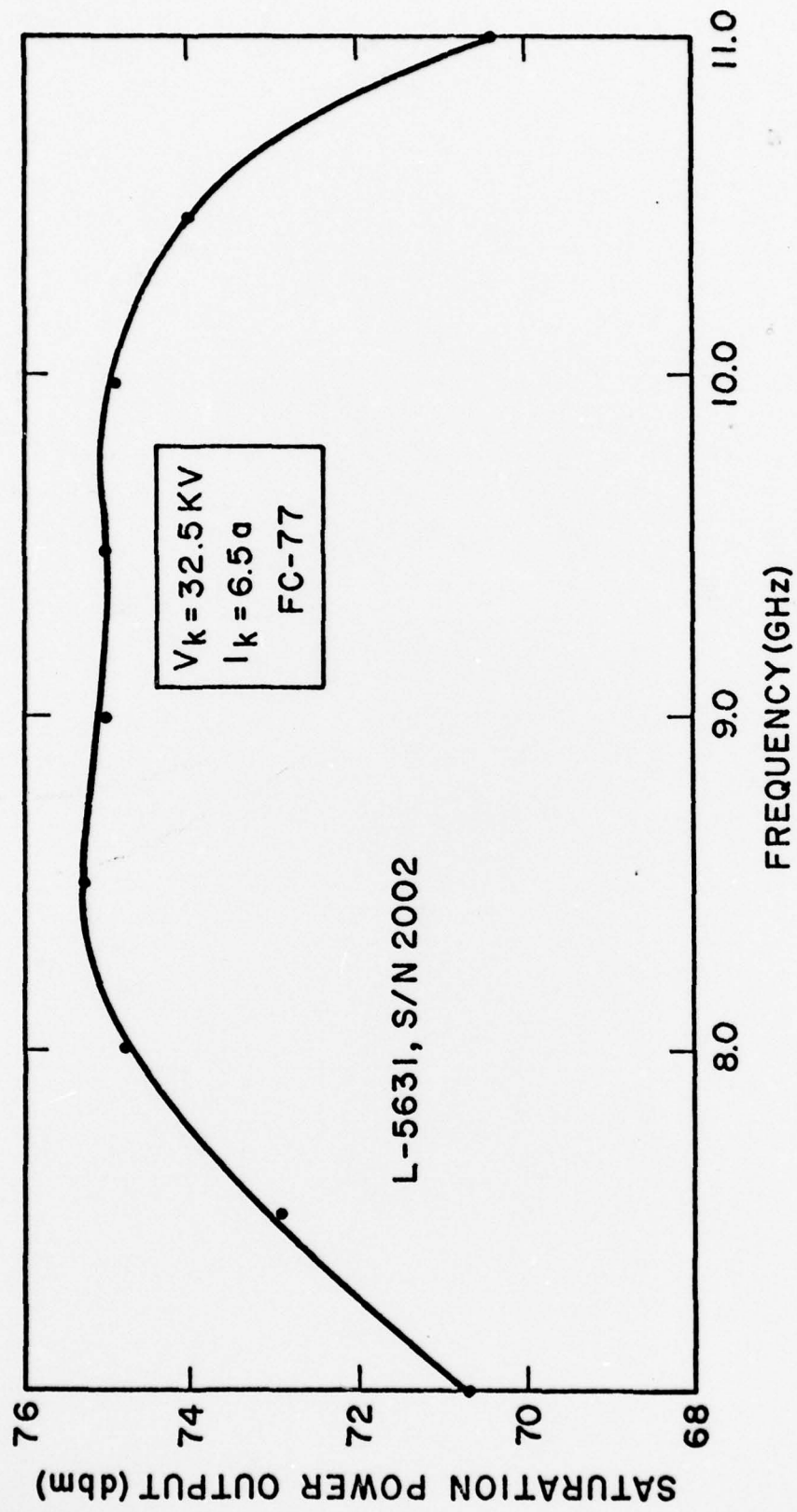
SATURATION POWER OUTPUT VS. FREQUENCY

FIG. 29
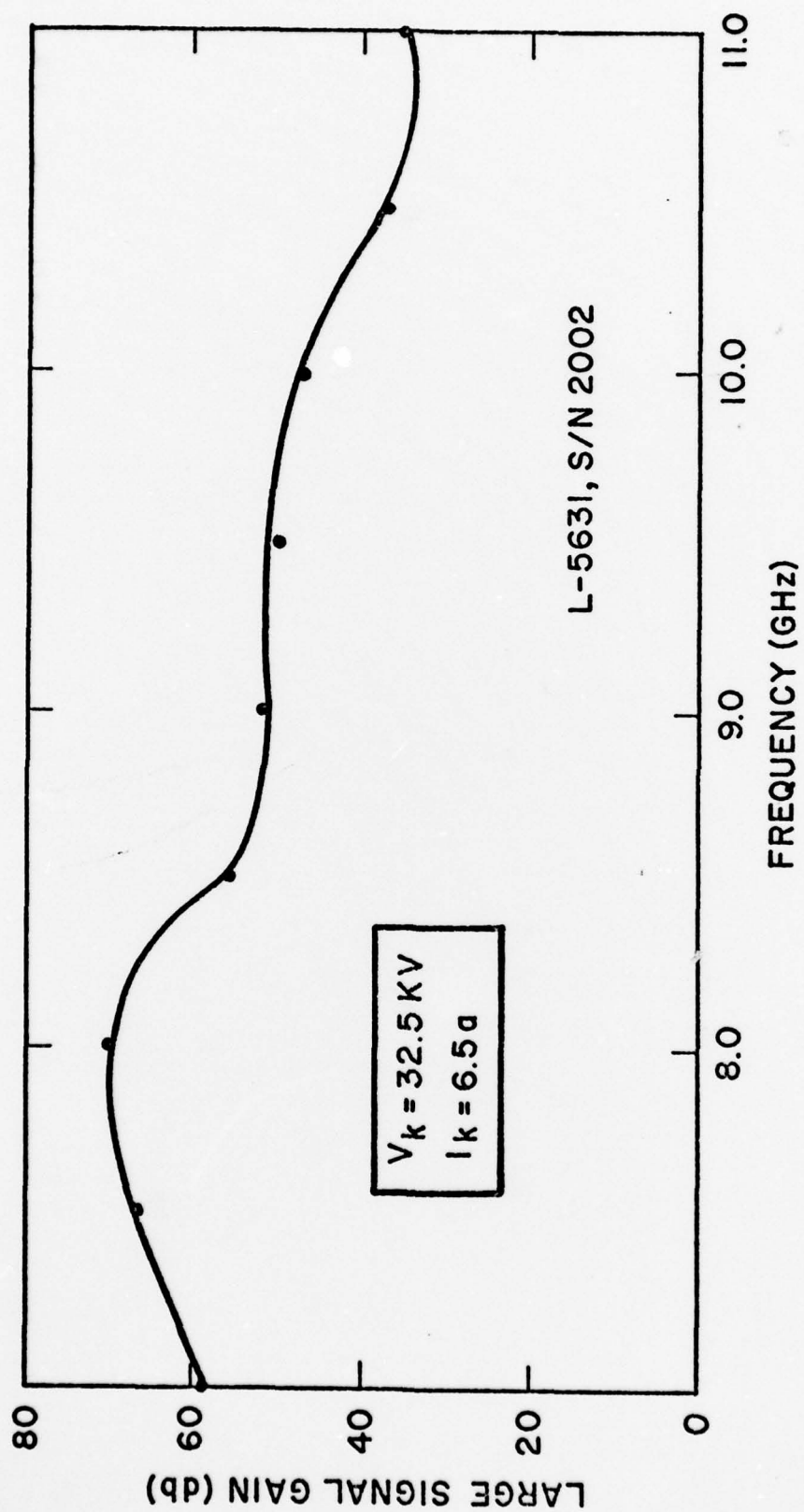
LARGE SIGNAL GAIN VS. FREQUENCY

FIG. 30

L-5631, S/N 2002

$V_k = 32.5$ KV
$I_k = 6.5$ a

FREQUENCY (GHz)

LARGE SIGNAL GAIN (db)

- 47 -
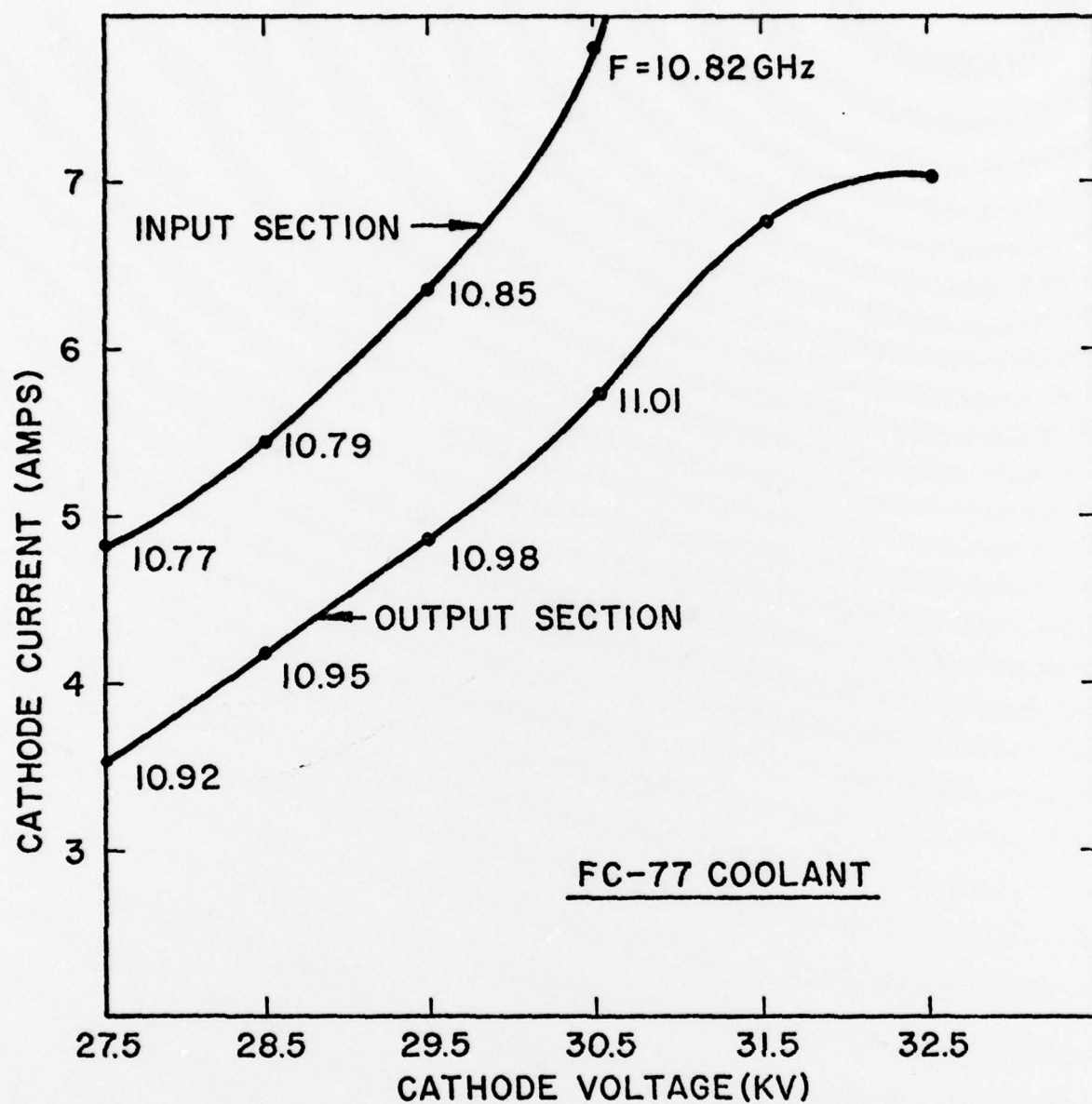
START OSCILLATION DATA
L-5631 S/N 2002

FIG. 31

8.0 CONCLUSIONS

Two wideband low AM-PM loss-line stabilized coupled cavity TWTs were built and demonstrated.

Both tubes were oscillation stable beyond the design current level.

The two tubes were of similar design and had similar electrical and RF performance.

The beam transmission characteristics were excellent, particularly for wideband tubes. Ninety-five percent transmission was measured without RF, 90% with RF.

The RF performance characteristics of these tubes are superior to current production loss button stabilized tubes. The RF efficiency is higher, particularly over the high frequency portion of the band. This is because the output sections of the loss line tubes are long enough to provide sufficient small signal gain between the circuit sever and the output cavity for good efficiency. For the same reason the AM-PM conversion for these tubes is better than the conventional loss button tubes. The gain variation across the frequency band is lower because of the high loss introduced at the low end of the band by the frequency selection attenuator sections. The RF duty factor is inherently higher because the loss lines are fluid cooled; (the RF power absorbed by the stabilization loss is a limiting duty factor for wideband tubes). The improved duty capability of the loss lines could not be demonstrated because the beam interception on the circuit was the duty limiting factor for these tubes. (The limiting duty factor of the loss lines could best be demonstrated in a solenoid version of this tube.)

Table II shows a comparison of the performance charac-
teristics for these tubes with the design objective.

The peak power specification was demonstrated over
most of the band (7.35 GHz - 10.75 GHz). Ten (10) kW
minimum was demonstrated at the bandedges, 7.0 GHz
and 11.0 GHz. The output power over 70% of the band
was flat within $\pm$ .5 dB.

The bandwidth and saturated gain exceeded the
specifications.

The AM-PM distortion objective specification of $.5^{\circ}$/dB
was not met. An average AM-PM of 1°/dB - 2°/dB from 7 - 10 GHz
was measured in the drive power region from saturation to
saturation minus 10 dB. The AM-PM conversion is less
for drive power greater than saturation and is higher
for frequencies above 10 GHz.

The efficiency specifications of 15% was met from
8.0 - 10.0 GHz and was 7% minimum at 7.0 and 11.0 GHz.

The stability of the tubes is adequate for operation in
the maximum bandwidth mode. The tubes can be under-
voltaged slightly (5%). At least 10% overvoltage is
possible. No regenerative oscillations were measured at
any voltage. The current stability is better than
6.5 amperes.

S/N 2001 was operated at high duty factor to evaluate the
average power capability of the loss lines. At 2% duty
factor there was less than .2 dB change in output power
fade at 11 GHz.

TABLE II

PERFORMANCE CHARACTERISTICS

Performance Parameter	Objective	Achieved	
		S/N 2001	S/N 2002
Peak Power	20 kW Min.	20 kW Min. (7.35 - 10.75 GHz) 10 kW Min. (7.0 and 11.0 GHz).	20 kW Min. (7.5 - 10.7 GHz) 10 kW Min. (7.0 and 11.0 GHz)
Bandwidth	40%	44%	44%
Frequency	X-Band	7 - 11 GHz	7 - 11 GHz
Saturated Gain	30 dB Min.	33 dB Min.	36 dB Min.
AM-PM Distortion (± 10 dB at Sat.)	.5°/dB	1°/dB-2°/dB Avg.(10dB underdrive). 7 - 10 GHz	-
Efficiency	15% Min.	17% Midband, 7% Min. (Bandedges).	15% Midband, 7% Min. (Bandedges).
Oscillation	± 5% beam voltage	+ 10% - 5%	+ 10% - 5%
Stability	+ 5% beam current	+ 33%	+ 7%
Duty	.01	.02	-

9.0 RECOMMENDATIONS FOR FUTURE WORK

Further development of loss line tubes should include:

1. Improved design of the in-band attenuators.

a) Provide higher attenuator loss for more gain equalization.

b) Develop more rigidly controlled reference loss distributions.

c) Develop more sophisticated taper sections to improve the match of the attenuators to the un-loaded sections of line.

2. Develop solenoid version to test limits of loss lines. Presently 2% duty limitation is a focusing limitation. The thermal limitation of the loss lines have not yet been established.

3. Qualification testing -- Tubes should be qualification tested to determine the suitability of the present mech-anical design. Shock and vibration testing is essential to insure that the present mechanical configuration of the loss lines is adequate.

10.0 REFERENCES

1. C. C. Cutler and D. J. Brangaccio, "Factors Affecting Traveling Wave Tube Power Capacity," IRE Trans. on Electron Devices, PGED-3, pp. 9-23 (June 1953).

2. A. Nordsieck, "Theory of large-signal behavior of traveling-wave amplifiers" Proc. IRE, vol 41, pp. 630-637, May, 1953.

3. A. Kiel and P. Parzen, "Nonlinear wave propagation in traveling-wave amplifiers," IRE Trans. Electron Devices, vol ED-2 pp. 26-34, Oct. 1955.

4. P. K. Tien, L. R. Walker and V. W. Wolontis, "A Large Signal Theory of Traveling Wave Amplifiers" Proc. IRE, vol. 43, pp. 260-277 (1955).

5. C. C. Cutler, "The Nature of Power Saturation in Traveling Wave Tubes," BSTJ, Vol. 35, pp. 841-876 (1956).

6. W. R. Beam and D. J. Blattner, "Phase Angle Distortion in Traveling Wave Tubes," RCA Rev., vol. 17, pp. 86-99 (1956).

7. J. P. Laico, H. L. McDowell, and C. R. Moster, "A medium power traveling-wave tube for 6,000 Mc radio relay," Bell Sys. Tech., vol. 35, pp. 1285-1346, 1956.

8. J. E. Rowe, "A large-signal analysis of the traveling-wave amplifier: Theory and general results," IRE Trans. Electron Devices, vol. ED-3, pp. 39-57, Jan. 1956.

9. C. K. Birdsall and C. C. Johnson, "Traveling Wave Tube Efficiency Degradation Due to Power Absorbed in an Attenuator," IRE Trans. on Electron Devices, ED-6, pp. 6-9 (Jan. 1959).

10. A. W. Scott, "Why a Circuit Sever Affects Traveling Wave Tube Efficiency," IRE Trans. on Electron Devices, Vol. ED-9, pp. 35-41 (Jan. 1962).

11. J. Ober, "The Large Signal Behavior of a Traveling Wave Tube With An Attenuating Central Helix Section," Philips Res. Rept., vol. 20, pp. 357-376 (1965).

12. J. I. Lindstrom, "Measurements of Nonlinearities in a Traveling Wave Tube," Internatl. J. Electronics, vol. 21, pp. 425-441 (1966).

13. O. Nilsson, "Nonlinear distortion in traveling-wave tubes," Chalmers Univ. of Tech., Sweden, Research Rep. 67, 1966.

14. A. J. Sangster, "Traveling-wave interactions in structures with nonzero impedance at harmonics of the driving frequency," presented at the 6th Int. Conf. Microwave and Optical Generation and Amplification, Cambridge, England, Sept. 1966.

References (continued)

15. M. E. El-Shandwily and J. E. Rowe, "Multisignal transfer characteristics of a traveling-wave amplifier," Int. J. Electron. vol. 22, no. 5, pp. 461-476, 1967.

16. O. G. Sauseng and U. J. Pittack, "Theoretical and experimental phase distortion in studies on traveling-wave tubes," Hughes Aircraft Co. Tech. Rep. 46, 1969.

17. H. Nishihara and M. Terada, "Effects of Attenuator on the Nonlinear Phase and Distortion of a TWT," IEEE Trans. - Ed., pp. 638-640 (1970).

18. N. J. Dione, "Harmonic generation in octave bandwidth traveling-wave tubes," IEEE Trans. Electron Devices, vol. ED-17, pp. 365-372, Apr. 1970.

19. H. Arnett, S. Smith and L. Winslow, "Design Concepts for Dual-Mode TWT," WRL Memorandum Report 2599, Naval Research Laboratory, Wash. D. C. (May 1973).

20. E. Ezura and T. Kano, "Measured and Theoretical Nonlinear Phase Distortion in Traveling-Wave Tubes," IEEE Trans. Electron Devices, vol. ED-22, pp. 890-897, Oct. 1975.

21. J. R. M. Vaughan, "Calculation of Coupled-Cavity TWT Performance" IEEE Trans. on Electron Devices, ED-22, pp. 880-890 (Oct. 1975).